THE PENETRATION OF A FINGER INTO A VISCOUS FLUID

Thesis by
Douglas Alan Reinelt

In Partial Fulfillment of the Requirements
for the Degree of
Doctor of Philosophy

California Institute of Technology
Pasadena, California

1984

(Submitted June 9, 1983)

Acknowledgements

I wish to thank my advisor, Dr. Philip G. Saffman, for suggesting the topic of this thesis and for his guidance throughout its development. Working with him has been enjoyable, and his depth of knowledge and understanding continues to be an inspiration to me. I would also like to thank the students and faculty of the Applied Mathematics Department for many helpful discussions during my stay at Caltech, especially Dr. Bengt Fornberg and Luis Reyna.

Financial support was provided by Caltech in the form of Graduate Teaching Assistantships, Graduate Research Assistantships, and a Special Institute Fellowship. The use of the Caltech computing facilities and the Fluid Mechanics VAX 11/750 in the Applied Mathematics department has been invaluable in conducting this research.

I would also like to express gratitude to my family for their unwavering support. Finally, I wish to thank my wife, Jeanne, for her help in preparing this thesis. Her continuing love and encouragement have been a source of great strength.

Abstract

The steady-state shape of a finger penetrating into a region filled with a viscous fluid is examined. The two-dimensional and axisymmetric problems are solved using Stokes's equations for low Reynolds number flow. Since the viscosity of the fluid inside the finger is assumed to be negliglible in comparison with the viscosity of the fluid exterior to the finger, boundary conditions for a liquid-gas interface are applied on the free surface of the finger.

The two-dimensional case is solved analytically by using singular perturbation methods. Inner and outer expansions are developed in terms of the small parameter $\mu U/T$. An ordinary differential equation for the shape of the finger is solved numerically in order to determine the inner solution. The method of matched asymptotic expansions is used to match the inner and outer solutions.

To solve the fingering problem numerically, an initial guess for the shape of the finger is made by using the perturbation solution. Since the shape of the finger has been fixed, we are forced to drop one of the three boundary conditions on the curved interface. The normal-stress boundary condition is dropped. To solve the resulting problem, the domain is covered with a composite mesh. It is composed of a curvilinear grid which follows the curved interface, and a rectilinear grid parallel to the straight boundaries. These overlapping grids are stretched so that the number of grid points is greatest in regions where they are needed most. Interpolation equations connect the two grids. Finite difference methods are used to calculate the numerical solution.

The curved interface of the finger is expanded in terms of Tchebycheff polynomials and the known asymptotic behavior of the finger as $x \to -\infty$. Using the solution calculated on the fixed domain, the expansion of the interface, and the

normal-stress boundary condition, the correct shape of the finger is determined using Newton's method.

When the axisymmetric finger moves through the tube, a fraction m of the viscous fluid is left behind on the walls of the tube. The fraction m was measured experimentally by Taylor [15] as a function of the parameter $\mu U/T$. The numerical results show excellent agreement with the experimental results of Taylor.

Table of Contents

I. Introduction

We consider the penetration of a finger of fluid into a region which is initially filled with a fluid more viscous than that of the finger. The steady-state shape of the finger is studied. Two different geometries are examined: a finger moving in a Hele-Shaw cell and in a tube.

A Hele-Shaw cell is composed of two closely spaced parallel plates separated by a distance $2b$. The sides of the cell are a distance $2l$ apart, where $l >> b$. A finger, shaped like a tongue, moves through the Hele-Shaw cell with constant velocity U. The thickness of the tongue is $2\beta b$ and its width is $2\lambda l$, where the parameter β is equal to (thickness of finger)/(distance between plates) and the parameter λ is equal to (width of finger)/(width of cell).

The determination of the value of λ has been a subject of much interest. Experiments examining the shape of a finger in a Hele-Shaw cell have been performed by Saffman and Taylor [13] and Pitts [8]. It was found that unless the flow is very slow the value of λ is close to $\frac{1}{2}$. Since the three-dimensional problem is difficult to solve, the shape of the finger in the plane parallel to the plates is examined mathematically by averaging the velocity field in the direction between the plates. This leads to equations in which the components of the mean velocity in the plane parallel to the plates are given by

$$u = -\frac{b^2}{3\mu}\frac{\partial p}{\partial x} \qquad v = -\frac{b^2}{3\mu}\frac{\partial p}{\partial y}$$

where $2b$ is the distance between the plates and μ is the viscosity of the fluid. The finger moves parallel to the x-axis.

These equations are identical to the equations for a two-dimensional porous media, where $\frac{b^2}{3}$ is equal to the permeability of the medium; thus, there is an analogy between a finger in a Hele-Shaw cell and a finger in a porous media. In certain methods of oil recovery, water or steam is pumped into the ground to force the oil towards the wells. If the velocity of the water is too large, then fingers of water will penetrate the oil. A mixture of oil and water is then extracted from the well. To avoid this, it is important to understand the conditions which determine the shape of the fingers.

If the fluid is incompressible, then the velocity potential φ

$$u = \frac{\partial \varphi}{\partial x} \qquad v = \frac{\partial \varphi}{\partial y}$$

must satisfy Laplace's equation

$$\frac{\partial^2 \varphi}{\partial x^2} + \frac{\partial^2 \varphi}{\partial y^2} = 0$$

It is assumed that the viscosity of the fluid inside the finger is negligible when compared with the viscosity exterior to the finger. This allows us to solve for φ only in the region exterior to the finger. The boundary condition on the sides of the cell $y = \pm l$ is given by

$$\frac{\partial \varphi}{\partial y} = 0$$

On the surface of the finger, φ satisfies

$$\frac{\partial \varphi}{\partial n} = U \cos \vartheta$$

where ϑ is the angle between the x-axis and the outward normal to the interface. φ also satisfies

$$p_0 - p = \frac{3\mu}{b^2}\varphi = T\left(\frac{1}{R_1} + \frac{1}{R_2}\right)$$

where p_0 is the constant pressure inside the finger. R_1 is the radius of curvature in the plane parallel to the plates, and R_2 is the radius of curvature in the plane perpendicular to the plates. The curvature $1/R_2$ is much larger than $1/R_1$. This last condition on the interface has been a subject of controversy.

Saffman and Taylor [13] assumed that the surface tension T could be neglected ($T=0$) and were able to derive a closed form solution. This solution is used to test a numerical method and is given in section 3.3. They also found that the difference between the shape of the finger determined from their closed form solution and the shape observed from the experimental results is considerable unless λ is close to $\frac{1}{2}$. The parameter λ is not determined by their analysis.

McLean [7] has taken into account the effect of the surface tension T in his examination of the fingering problem. In his analysis, he has assumed that the value of R_2 is equal to a constant ($R_2 = b$). If R_2 is constant, then it is simply an additive constant to the velocity potential φ, and has no effect on the solution. The shape of the finger determined by McLean with a given value of λ is in close agreement with the shape given by experimental results with the same value of λ. A comparison between a plot of λ versus $\mu U/T$ using McLean's results and the same plot using the experimental results shows an appreciable difference between the two.

In an attempt to improve the agreement between the plots, Romero [11] has assumed that R_2 is a function of the normal velocity at the interface. Numerical results were calculated for $1/R_2$ proportional to the normal velocity at the interface and the square of the normal velocity. By using these interface conditions, Romero modified the plot of λ versus $\mu U/T$ in a way that was a

qualitative improvement over McLean's results when compared with the experimental plots. The actual dependence of R_2 as a function of the velocity was not known.

To better understand the relationship of R_2 to the velocity of the fluid, we examine the narrow shape of the finger that can be seen by looking between the two plates. The determination of the value of R_2 as a function of $\mu U/T$ can possibly be used to develop a better interface condition for the velocity potential φ and bring the plot of λ versus $\mu U/T$ in closer agreement with experiments.

If the distance $b << l$, then a two-dimensional approximation to the flow is valid. Stokes's equations for low Reynolds number flow are applied in the plane perpendicular to the plates and parallel to the x-axis. The *no-slip condition* is applied at the solid plates. Since the viscosity inside the finger is set equal to zero, the boundary conditions for a liquid-gas interface are used on the free surface of the finger.

The above problem is solved analytically by using singular perturbation methods. The inner and outer expansions are developed in terms of the small parameter $\mu U/T$. An ordinary differential equation for the shape of the finger needs to be solved numerically at each order of the inner solution. The method of matched asymptotic expansions is used to show that the inner and outer solutions match in an appropriate overlap region. In addition to the perturbation solution, a solution as $x \to -\infty$ is found in terms of an eigenfunction expansion. This leads to a relationship between β, $\mu U/T$, and k, the exponential decay rate at which the shape of the finger asymptotes to its constant value. These analytical results are compared with the numerical results.

To solve the fingering problem numerically, we begin with an initial guess for the correct shape of the finger. This can be found by starting with a small

value for the parameter $\mu U/T$ and using the perturbation solution. Since we have fixed the shape of the finger, we are forced to drop one of the three boundary conditions applied on the curved interface. The normal-stress boundary condition is dropped. A system of equations equivalent to the biharmonic equation must now be solved on a fixed domain. It is important to use a numerical method that not only gives accurate results in the interior of the domain but also gives accurate results on the curved interface. To accomplish this, we use a composite mesh to cover the domain. It is composed of a rectilinear grid, which is parallel to the straight boundaries, and a curvilinear grid, which follows the curved interface. These overlapping grids are stretched so that the number of grid points is greatest in regions where they are needed most. Interpolation equations are used to connect the two grids. Finite difference methods are used to calculate the numerical solution.

The curved interface of the finger is expanded in terms of Tchebycheff polynomials and the known asymptotic behavior of the finger as $x \to -\infty$. Using the solution calculated on the fixed domain, the expansion of the interface, and the normal-stress boundary condition, a new shape for the interface is determined by Newton's method. After several iterations, the normal-stress boundary condition is satisfied.

The numerical results agree with the perturbation solution for very small values of $\mu U/T$. A comparison of the numerical and analytic results in regard to the relationship between β, $\mu U/T$, and k, determined from the eigenfunction expansion as $x \to -\infty$, shows agreement for a larger range of $\mu U/T$.

The numerical methods used for the two-dimensional problem are applied to the penetration of a finger into a viscous fluid in a tube. The diameter of the tube is $2b$ and the diameter of the finger moving through the tube with

constant velocity U is $2\beta b$. The parameter β is equal to (diameter of finger)/(diameter of tube). When the axisymmetric finger moves through the tube, a fraction m of the viscous fluid is left behind on the walls of the tube. The value of m is related to β by $m = 1-\beta^2$. The fraction m was measured experimentally by Taylor [15] as a function of the parameter $\mu U/T$. The numerical results are nearly identical with the experimental results of Taylor.

II. Analytic Solutions of the Fingering Problem

2.1 Formulation of the Problem

We consider the penetration of a finger of fluid into the narrow region between two closely spaced parallel plates. The region between the plates is initially filled with a fluid more viscous than that of the finger. The steady state problem is examined where the finger is moving with constant velocity U. The plates are separated by a distance $2b$ and the finger has width $2\beta b$ (see Figure 1).

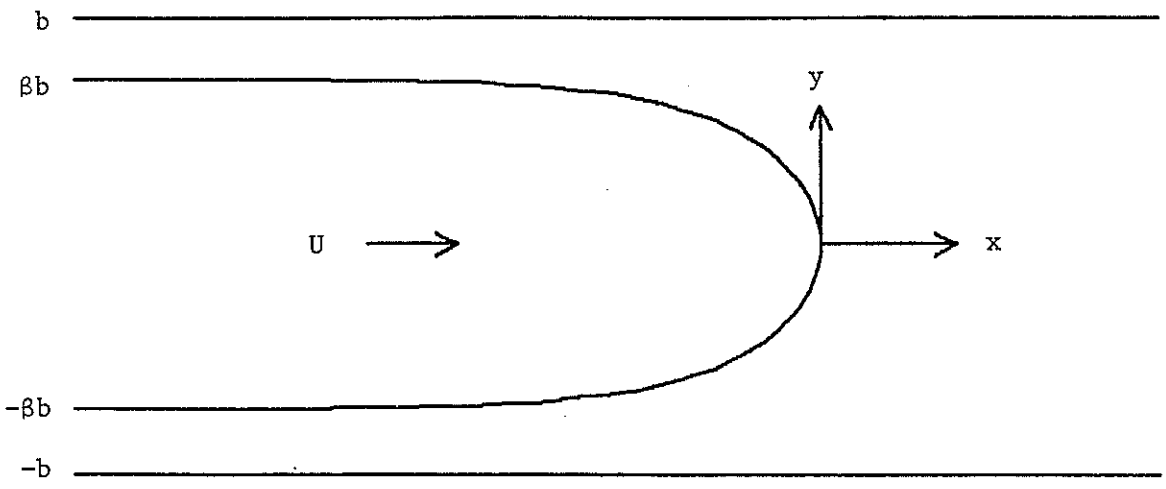

Figure 1

We examine the flow in a plane perpendicular to the plates. If the distance $2b$ is much smaller than the dimensions of the plates, then a two-dimensional approximation to the flow is valid. The conservation and momentum equations for incompressible two-dimensional flow are

$$u_x + v_y = 0$$
$$\rho(u_t + uu_x + vu_y) = -p_x + \mu(u_{xx} + u_{yy}) \qquad (1a,b,c)$$
$$\rho(v_t + uv_x + vv_y) = -p_y + \mu(v_{xx} + v_{yy})$$

where p is the pressure, μ is the viscosity, and ρ is the density of the fluid. The velocities u and v of the fluid are in the x and y direction respectively. The tip of the finger moves along the x-axis.

Boundary conditions must be applied on the plates $y = \pm b$ and on the interface between the two fluids. On the solid boundaries, the *no-slip condition* is applied. To find the appropriate interface conditions, it is assumed that the viscosity of the fluid inside the finger is negligible when compared with the viscosity of the fluid exterior to the finger. For example, a finger of air being blown into glycerine. This allows us to solve equations (1a,b,c) only in the region exterior to the finger and to use the boundary conditions for a liquid-gas interface. It is also assumed that the fluids remain completely separated along the interface; thus, the relative velocity normal to the interface must be equal to zero. The other two boundary conditions for a liquid-gas interface come from balancing the difference in stress across the interface to the normal force due to surface tension. Let $\mathbf{n} = (n_x, n_y)$ be the normal vector to the interface pointing into the finger and $\mathbf{t} = (t_x, t_y)$ be the tangent vector to the interface. The three boundary conditions that must be satisfied on the interface are

$$(u - U)n_x + vn_y = 0$$
$$u_x t_x n_x + \frac{1}{2}(u_y + v_x)(t_x n_y + t_y n_x) + v_y t_y n_y = 0$$
$$p - 2\mu[u_x n_x^2 + (u_y + v_x)n_x n_y + v_y n_y^2] = p_0 - \frac{T}{R}$$

where p_0 is the constant pressure inside the finger, T is the surface tension, and R is the radius of curvature.

We now change to a reference frame moving with the finger. The tip of the finger is fixed at the origin. In this new reference frame, the velocities are independent of time. Dimensionless variables are introduced by

$$\hat{x} = \frac{x - Ut}{b} \qquad \hat{y} = \frac{y}{b} \qquad \hat{R} = \frac{R}{b}$$

$$\hat{u} = \frac{u - U}{U} \qquad \hat{v} = \frac{v}{U} \qquad \hat{p} = \frac{p}{T/b}$$

In the perturbation analysis of the fingering problem, it becomes clear that the appropriate scaling for p is T/b and not $\mu U/b$. We substitute these new variables into equations (1a,b,c) to get

$$\hat{u}_{\hat{x}} + \hat{v}_{\hat{y}} = 0$$

$$\left[\frac{\rho U b}{\mu}\right](\hat{u}\hat{u}_{\hat{x}} + \hat{v}\hat{u}_{\hat{y}}) = -\left[\frac{T}{\mu U}\right]\hat{p}_{\hat{x}} + \hat{u}_{\hat{x}\hat{x}} + \hat{u}_{\hat{y}\hat{y}}$$

$$\left[\frac{\rho U b}{\mu}\right](\hat{u}\hat{v}_{\hat{x}} + \hat{v}\hat{v}_{\hat{y}}) = -\left[\frac{T}{\mu U}\right]\hat{p}_{\hat{y}} + \hat{v}_{\hat{x}\hat{x}} + \hat{v}_{\hat{y}\hat{y}}$$

We make the further assumption that the inertia terms can be neglected in comparison with the viscous terms. This implies that the Reynolds number is much less than one ($\mathrm{Re} = \rho U b/\mu << 1$). We drop the hats in the above equations to get

$$\begin{aligned} u_x + v_y &= 0 \\ p_x &= Ca\,(u_{xx} + u_{yy}) \\ p_y &= Ca\,(v_{xx} + v_{yy}) \end{aligned} \qquad \text{(2a,b,c)}$$

where $Ca = \mu U/T$. The capillary number Ca is the ratio of the viscous force to the force of surface tension. The parameter β, which is the ratio of the width of the finger to the distance between the plates, is a function of the capillary number.

Since it is assumed that the shape of the finger is symmetric in the y direction, it is only necessary to solve equations (2a,b,c) for $y \geq 0$. The symmetry conditions on the centerline $y = 0$ are

$$u_y(x,0) = 0 \qquad v(x,0) = 0 \tag{3a,b}$$

Figure 2 gives the new geometry for the problem.

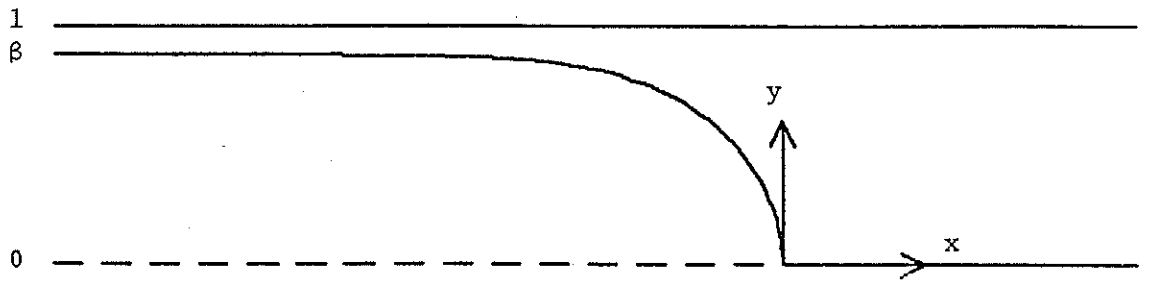

Figure 2

In the new reference frame, the *no-slip condition* becomes

$$u(x,1) = -1 \qquad v(x,1) = 0 \tag{4a,b}$$

and the boundary conditions on the interface become

$$\begin{aligned} un_x + vn_y &= 0 \\ u_x t_x n_x + \tfrac{1}{2}(u_y + v_x)(t_x n_y + t_y n_x) + v_y t_y n_y &= 0 \\ p - 2\,Ca\,[u_x n_x^2 + (u_y + v_x)\,n_x n_y + v_y n_y^2] &= p_0 - \frac{1}{R} \end{aligned} \tag{5a,b,c}$$

Since the pressure can only be determined up to a constant, we are free to set the pressure inside the finger equal to zero.

It is important to know the behavior of the solution as $x \to \pm\infty$. As $x \to -\infty$, the width of the finger approaches a constant; thus, we get a constant velocity between the finger and the solid boundary. Pouseuille flow develops as $x \to \infty$.

$$u \to -1 \quad \text{and} \quad v \to 0 \quad \text{as} \quad x \to -\infty$$

$$u \to \frac{3}{2}\beta(1-y^2)-1 \quad \text{and} \quad v \to 0 \quad \text{as} \quad x \to \infty$$

2.2 Perturbation Solution

In this section, we treat the penetration of a finger into a viscous fluid as a singular perturbation problem. The solution is expanded in terms of the dimensionless parameter δ . The parameter δ is a convenient length scale in the narrow region between the finger and the wall and is related to the capillary number by $\delta = Ca^{\frac{2}{3}}$. An outer expansion is developed in terms of the primary reference variables in the problem. Dimensionless inner variables are found by stretching the primary reference variables by appropriate functions of the dimensionless parameter. These inner variables are now of order unity in the region of nonuniformity of the outer expansion. An inner expansion is developed and matched to the outer expansion by the method of matched asymptotic expansions. A more detailed explanation of singular perturbation methods in fluid flow can be found in Van Dyke [16].

This analysis of the penetration of a finger into a viscous fluid is related to the work of Bretherton [2] and his analysis of the motion of long bubbles in tubes. This work differs from Bretherton's work in that it outlines a procedure to develop a complete asymptotic expansion in terms of δ . It also constructs the equations properly in the boundary layer region in terms of scaled coordinates of order unity. The method of matched asymptotic expansions is used to show that the outer and inner solutions match in an appropriate overlap region.

In the perturbation problem, the interface is best described as a function of x. If $y = h(x)$ is the equation for the interface, then the interface conditions (5a,b,c) are

$$v = h_x u$$

$$0 = (u_y + v_x)(1 - h_x^2) - 4 u_x h_x \qquad \text{(6a,b,c)}$$

$$p = -Ca\,[2 u_x + h_x (u_y + v_x)] + h_{xx}[1 + h_x^2]^{-\frac{3}{2}}$$

The equations have been simplified by using the continuity equation (2a) and by adding part of equation (5b) to equation (5c).

To get the leading order term in the outer expansion, we let $Ca \to 0$ in equations (2a,b,c). The simplified version of these equations is given by

$$p_x^0 = 0 \qquad p_y^0 = 0$$

This implies that the leading order approximation to the pressure, $p^0(x,y)$ is a constant. To determine the constant, we examine the interface condition (6c) as $Ca \to 0$

$$p^0 = -\frac{1}{R^0} = h_{xx}^0 [1 + (h_x^0)^2]^{-\frac{3}{2}}$$

From this equation, the leading order term of the radius of curvature is also equal to a constant. In the limit as $Ca \to 0$, the finger fills the entire region between the two plates ($\beta \to 1$). The angle of contact at the wall must be zero; thus, $R^0 = 1$. The leading order approximations to the pressure and to $h(x)$ in the outer expansion are given by

$$p^0 = -1 \qquad h^0(x) = \sqrt{1 - (x+1)^2} \qquad \text{(7a,b)}$$

Before finding higher order terms in the outer region, we first examine the

equations in the inner region.

In the inner transition region, the dependent and independent variables must be scaled so that the new variables are of order unity. The region of nonuniformity of the outer solution is located near $(x,y)=(-1,1)$ where the free surface given by the outer solution contacts the wall. Let $d=1-\beta$ be the distance between the finger and the wall as $x \to -\infty$. We introduce the parameter δ as a length scale for the distance d. The parameter δ is related to the original parameter Ca by $Ca=\delta^m$ where m must be determined. Clearly, $y-1$ and $h-1$ are of the same order as d in the inner region and thus must be scaled by δ. The new x coordinate is centered at the position where the interface, determined by the leading order outer solution, contacts the wall; thus, we expect the form $(x+1)/\delta^n$ for this inner coordinate. In the inner region, $\frac{dh}{dx}$ is much less than 1 as $\delta \to 0$ which implies $0 < n < 1$.

The inner variables for the velocities are given by $(u+1)/\delta^k$ and v/δ^{k+1-n}. The scaling for the velocity v is chosen such that both terms in the continuity equation (2a) are of the same order. The pressure p is asymptotic to -1 in the outer region and is equal to 0 as $x \to -\infty$; thus, the pressure is already $O(1)$ in the inner region.

If the inner variables are given by $\bar{x}$, $\bar{y}$, $\bar{h}$, $\bar{u}$, $\bar{v}$, and $\bar{p}$, then boundary condition (6a) is written in terms of these variables by

$$\delta^k \bar{v} = \bar{h}_{\bar{x}} \left(-1+\delta^k \bar{u}\right)$$

Since $\bar{h}_{\bar{x}}$ is not equal to 0 in the inner region, the value of k must be equal to 0; thus, it is not necessary to scale u in the inner region. Equation (2b) is given by

$$\bar{p}_{\bar{x}} = \delta^{m-n} \bar{u}_{\bar{x}\bar{x}} + \delta^{m+n-2} \bar{u}_{\bar{y}\bar{y}}$$

Since n is less than 1, the coefficient in front of $\bar{u}_{\bar{y}\bar{y}}$ is the larger of the two coefficients; $\bar{u}_{\bar{y}\bar{y}}$ must balance with the pressure term. This implies that $m+n-2=0$ and $m-n>0$. Finally, boundary condition (6c) is given in terms of the inner variables by

$$\bar{p} = -\delta^{m-n}\left[2\bar{u}_{\bar{x}} + \bar{h}_{\bar{x}}\left(\bar{u}_{\bar{y}} + \delta^{2-2n}\bar{v}_{\bar{x}}\right)\right] + \delta^{1-2n}\bar{h}_{\bar{x}\bar{x}}\left(1+\delta^{2-2n}\bar{h}_{\bar{x}}^2\right)^{-\frac{3}{2}}$$

Since $m-n>0$, the pressure term can only balance with $\bar{h}_{\bar{x}\bar{x}}$. This gives $n=\frac{1}{2}$ and $m=2-n=\frac{3}{2}$, which completes the determination of the inner variables.

The inner variables can now be written as

$$\bar{x} = \frac{x+1}{\delta^{\frac{1}{2}}} \qquad \bar{y} = \frac{y-1}{\delta} \qquad \bar{h} = \frac{h-1}{\delta}$$
$$\bar{u} = u \qquad \bar{v} = \frac{v}{\delta^{\frac{1}{2}}} \qquad \bar{p} = p \tag{8}$$

and the new parameter δ is related to the original parameter Ca by $Ca=\delta^{\frac{3}{2}}$. Substitution of the inner variables (8) into equations (2a,b,c) gives

$$\bar{u}_{\bar{x}} + \bar{v}_{\bar{y}} = 0$$
$$\bar{p}_{\bar{x}} = \delta\bar{u}_{\bar{x}\bar{x}} + \bar{u}_{\bar{y}\bar{y}} \tag{9a,b,c}$$
$$\bar{p}_{\bar{y}} = \delta^2\bar{v}_{\bar{x}\bar{x}} + \delta\bar{v}_{\bar{y}\bar{y}}$$

In terms of the inner variables, the boundary conditions (4a,b) become

$$\bar{u}(\bar{x},0) = -1 \qquad \bar{v}(\bar{x},0) = 0 \tag{10a,b}$$

and the interface conditions (6a,b,c) evaluated on $\bar{y}=\bar{h}(\bar{x})$ become

$$\bar{v} = \bar{h}_{\bar{x}}\bar{u}$$

$$0 = (\bar{u}_{\bar{y}} + \delta\bar{v}_{\bar{x}})(1-\delta\bar{h}_{\bar{x}}^2) - 4\delta\bar{u}_{\bar{x}}\bar{h}_{\bar{x}} \qquad (11a,b,c)$$

$$\bar{p} = -2\delta\bar{u}_{\bar{x}} - (\delta\bar{u}_{\bar{y}} + \delta^2\bar{v}_{\bar{x}})\bar{h}_{\bar{x}} + \bar{h}_{\bar{x}\bar{x}}(1+\delta\bar{h}_{\bar{x}}^2)^{-\frac{3}{2}}$$

Setting δ equal to zero gives us the leading order approximations to the inner equations. The following versions of equations (9), (10), and (11) result:

$$\bar{u}_{\bar{x}}^0 + \bar{v}_{\bar{y}}^0 = 0$$

$$\bar{p}_{\bar{x}}^0 = \bar{u}_{\bar{y}\bar{y}}^0 \qquad (12a,b,c)$$

$$\bar{p}_{\bar{y}}^0 = 0$$

$$\bar{u}^0(\bar{x},0) = -1$$

$$\bar{v}^0(\bar{x},0) = 0 \qquad (13a,b)$$

$$\bar{v}^0(\bar{x},\bar{h}^0) = \bar{h}_{\bar{x}}^0\bar{u}^0(\bar{x},\bar{h}^0)$$

$$0 = \bar{u}_{\bar{y}}^0(\bar{x},\bar{h}^0) \qquad (14a,b,c)$$

$$\bar{p}^0(\bar{x},\bar{h}^0) = \bar{h}_{\bar{x}\bar{x}}^0$$

This system of equations can now be solved. The following solutions of equations (12a,b,c) satisfy all of the boundary conditions except conditions (14a) and (14c):

$$\bar{p}^0(\bar{x},\bar{y}) = P^0(\bar{x})$$

$$\bar{u}^0(\bar{x},\bar{y}) = \tfrac{1}{2}P_{\bar{x}}^0(\bar{x})[\bar{y}^2 - 2\bar{y}\,\bar{h}^0] - 1 \qquad (15a,b,c)$$

$$\bar{v}^0(\bar{x},\bar{y}) = P_{\bar{x}\bar{x}}^0(\bar{x})[-\tfrac{1}{6}\bar{y}^3 + \tfrac{1}{2}\bar{y}^2\bar{h}^0] + P_{\bar{x}}^0(\bar{x})[\tfrac{1}{2}\bar{y}^2\bar{h}_{\bar{x}}^0]$$

These three solutions still have two unknown functions, $P^0(\bar{x})$ and $\bar{h}^0(\bar{x})$. Substitution of the velocity solutions (15b,c) into the boundary condition (14a) leaves us with an equation for P^0 and $\bar{h}^0$.

$$P^0_{\bar{x}\bar{x}}(\bar{h}^0)^3 + 3P^0_{\bar{x}}(\bar{h}^0)^2\bar{h}^0_{\bar{x}} = -3\bar{h}^0_{\bar{x}}$$

This equation can now be integrated once and combined with the boundary condition (14c) to give an equation for $\bar{h}^0$

$$\bar{h}^0_{\bar{x}\bar{x}\bar{x}} = \frac{-3(\bar{h}^0+\bar{d})}{(\bar{h}^0)^3} \tag{16}$$

where the constant of integration is given by $\bar{h}^0 \to -\bar{d}$ as $\bar{x} \to -\infty$. Equation (16) is an ordinary differential equation for $\bar{h}^0$ that is solved numerically.

In order to integrate equation (16) numerically, the asymptotic solution as $\bar{x} \to -\infty$ is determined. This leads to a solution with three independent constants as expected. Two of these constants multiply exponentially growing solutions as $\bar{x} \to -\infty$ and must be discarded. The third constant is written as a translation in $\bar{x}$ since equation (16) is an autonomous equation. The resulting asymptotic behavior is

$$\bar{h}^0(\bar{x}) \sim -\bar{d}\left[1+\exp\left[\frac{3^{\frac{1}{3}}(\bar{x}+\bar{x}_0)}{\bar{d}}\right]-\frac{3}{7}\exp\left[\frac{2\cdot 3^{\frac{1}{3}}(\bar{x}+\bar{x}_0)}{\bar{d}}\right]+\cdots\right]$$

If we now make the change of variables

$$\hat{h} = \frac{\bar{h}^0}{\bar{d}} \qquad \hat{x} = \frac{3^{\frac{1}{3}}(\bar{x}+\bar{x}_0)}{\bar{d}}$$

then as $\hat{x} \to -\infty$

$$\hat{h}(\hat{x}) \sim -1-\exp(\hat{x})+\frac{3}{7}\exp(2\hat{x})+\cdots \tag{17}$$

and (16) becomes

$$\hat{h}_{\hat{x}\hat{x}\hat{x}} = \frac{-(\hat{h}+1)}{\hat{h}^3} \tag{18}$$

In order to match to the outer solution, it is necessary to find the asymptotic expansion of equation (18) as $\hat{x} \to \infty$. This asymptotic behavior is given by

$$\hat{h}(\hat{x}) \sim a\,\hat{x}^2 + b\,\hat{x} + c + O\left(\frac{1}{\hat{x}}\right) \tag{19}$$

The unknown constants a, b, and c are determined by numerical intergration of equation (18) with the initial condition (17). The results are

$$a = -0.3125 \qquad b = -0.096 \qquad c = -2.9$$

Transforming equation (19) back to inner variables gives

$$\bar{h}^0(\bar{x}) \sim \frac{a\,3^{\frac{2}{3}}(\bar{x}+\bar{x}_0)^2}{\bar{d}} + b\,3^{\frac{1}{3}}(\bar{x}+\bar{x}_0) + c\,\bar{d} + O\left(\frac{1}{\bar{x}}\right) \tag{20}$$

The method of matched asymptotic expansions requires that the inner solution as $\bar{x} \to \infty$ match with the outer solution as $x \to -1$. The matching can be done using an intermediate variable between x and $\bar{x}$ or more simply in terms of the original variables. In outer variables, equation (20) becomes

$$\begin{aligned} h^0(x) \sim 1 + \frac{a\,3^{\frac{2}{3}}(x+1)^2}{\bar{d}} + \delta^{\frac{1}{2}}\left(\frac{2a\,3^{\frac{2}{3}}\bar{x}_0}{\bar{d}} + b\,3^{\frac{1}{3}}\right)(x+1) \\ + \delta\left(\frac{a\,3^{\frac{2}{3}}\bar{x}_0^2}{\bar{d}} + b\,3^{\frac{1}{3}}\bar{x}_0 + c\,\bar{d}\right) + O(\delta^{\frac{3}{2}}) \end{aligned} \tag{21}$$

and the asymptotic behavior of (7b) as $x \to -1$ becomes

$$h^0(x) \sim 1 - \frac{1}{2}(x+1)^2 + O((x+1)^4) \tag{22}$$

Since we only have the leading order behavior of the inner and outer solutions, only the first two terms of (21) and (22) can be matched. This determines the

value of $\bar{d}$.

$$\bar{d} = -2\alpha 3^{\frac{2}{3}} = 1.3375$$

To determine $\bar{x}_0$, the other unknown constant in the leading order behavior of the inner solution, it is necessary to examine the next term in the outer solution.

To develop a complete expansion, the dependent variables are expanded in a series in powers of $\delta^{\frac{1}{2}}$.

$$\begin{aligned} p &= p^0+\delta^{\frac{1}{2}}p^1+\delta p^2+\delta^{\frac{3}{2}}p^3+\cdots \\ u &= u^0+\delta^{\frac{1}{2}}u^1+\delta u^2+\cdots \\ v &= v^0+\delta^{\frac{1}{2}}v^1+\delta v^2+\cdots \\ h &= h^0+\delta^{\frac{1}{2}}h^1+\delta h^2+\cdots \end{aligned}$$

Substituting these expansions into (2a,b,c) with $Ca = \delta^{\frac{3}{2}}$, we find that both p^1 and p^2 are also equal to a constant. From the interface boundary condition (6c), the radius of curvature is also a constant up to order δ. This leads to the following equations for $h^1(x)$:

$$h^1(x) = \frac{-r_1 x}{\sqrt{1-(x+1)^2}} \tag{23}$$

and as $x \to -1$,

$$h^1(x) \sim r_1 - r_1(x+1) + O((x+1)^2) \tag{24}$$

Comparing equation (24) with the $O(\delta^{\frac{1}{2}})$ terms in the inner expansion of equation (21), we find that the inner and outer expansions can only be matched if

$\tau_1 = 0$. This implies that $h^1(x) = 0$. The coefficient of the $O(\delta^{\frac{1}{2}})$ term in the inner expansion must also be set equal to zero. This determines the value of $\bar{x}_0$.

$$\bar{x}_0 = -\frac{\bar{d}\, b}{2\cdot(3)^{\frac{1}{3}} a} = -0.138$$

The second term in the outer expansion is thus $O(\delta)$ and not $O(\delta^{\frac{1}{2}})$. Since the $O(\delta^{\frac{1}{2}})$ vanished, the expression for $h^2(x)$ is equivalent to (23) and (24) with τ_1 replaced by τ_2. Matching with the inner expansion determines τ_2.

$$\tau_2 = \left[\frac{a\, 3^{\frac{2}{3}} \bar{x}_0^2}{\bar{d}} + b\, 3^{\frac{1}{3}} \bar{x}_0 + c\bar{d} \right] = -3.9$$

We could now continue by expanding the inner variables $\bar{u}$, $\bar{v}$, $\bar{p}$, and $\bar{h}$ in powers of $\delta^{\frac{1}{2}}$. An ordinary differential equation would appear at each order that could be solved numerically. The asymptotic expansion of these solutions as $\bar{x} \to \infty$ would be matched to the outer solution as $x \to -1$.

In summary, we have found

$$\beta \sim 1.0 - 1.3375 \left(\frac{\mu U}{T} \right)^{\frac{2}{3}}$$

$$R \sim 1.0 - 3.9 \left(\frac{\mu U}{T} \right)^{\frac{2}{3}} \qquad \text{(25a,b,c)}$$

$$p \sim -1.0 - 3.9 \left(\frac{\mu U}{T} \right)^{\frac{2}{3}}$$

Unfortunately, the expansions for the inner and outer variables are in powers of $(\mu U / T)^{\frac{1}{3}}$. This means that unless $\mu U / T$ is very small the errors from the terms

left out cannot be neglected. The above expressions will be compared with the numerical results.

2.3 Analytic Solution as $x \to -\infty$

Instead of using the formal perturbation expansion in the parameter δ, we expand the solution as $x \to -\infty$ in powers of $\exp(kx)$. This will give us a relationship between k, the decay rate as $x \to -\infty$, d, the distance between the finger and the wall as $x \to -\infty$, and $Ca = \mu U/T$. The relationship is valid for arbitrary Ca, unlike the solution in section 2.2 which was only valid for very small values of Ca.

The velocities and pressure take the form

$$u(x,y) \sim -1 + e^{kx} f(y) + O(e^{2kx})$$
$$v(x,y) \sim e^{kx} g(y) + O(e^{2kx})$$
$$p(x,y) \sim Ca\, e^{kx} h(y) + O(e^{2kx})$$

Substituting the above expressions into equations (2a,b,c) and eliminating two of the unknown functions, we get an equation for $g(y)$.

$$g_{yyyy} + 2k^2 g_{yy} + k^4 g = 0$$

The solution to this equation is a combination of the functions $\sin(ky)$, $\cos(ky)$, $y\sin(ky)$, and $y\cos(ky)$. The functions $f(y)$ and $h(y)$ are found in terms of $g(y)$. If we satisfy the boundary conditions on the wall (4a,b) then the velocities, pressure, and shape of the interface are

$$u(x,y) \sim -1 + e^{kx}\Big[A[-k(y-1)\sin(k(y-1))] + B[\sin(k(y-1)) + k(y-1)\cos(k(y-1))]\Big]$$

$$v(x,y) \sim e^{kx}\Big\{A[-k(y-1)\cos(k(y-1))+\sin(k(y-1))] + B[-k(y-1)\sin(k(y-1))]\Big\}$$

$$p(x,y) \sim Ca\, e^{kx}\Big\{A[-2k\cos(k(y-1))]+B[-2k\sin(k(y-1))]\Big\}$$

$$h(x) \sim \beta - D\, e^{kx}$$

where A, B, and D are unknown constants. The above expressions are substituted into the interface boundary conditions (6a,b,c). If we keep only terms of $O(\exp(kx))$, then the three equations for A, B, and D are given by the matrix equation

$$\begin{bmatrix} -k\,d\cos(kd)+\sin(kd) & k\,d\sin(kd) & k \\ 2k^2 d\cos(kd) & 2k\cos(kd)-2k^2 d\sin(kd) & 0 \\ Ca\,(2k\cos(kd)+2k^2 d\sin(kd)) & 2\,Ca\,k^2 d\cos(kd) & -k^2 \end{bmatrix} \begin{bmatrix} A \\ B \\ D \end{bmatrix} = \begin{bmatrix} 0 \\ 0 \\ 0 \end{bmatrix}$$

where $d = 1-\beta$. The determinant of the matrix must be set equal to zero for a solution other than the trivial solution. This leads to an equation for $q = k\,d$

$$2q - \sin(2q) + Ca\,(4q^2 - 4\cos^2 q) = 0 \qquad (26)$$

The asymptotic solution of equation (26) as $Ca \to 0$ is given by

$$k \sim \frac{(3\,Ca)^{\frac{1}{3}}}{d} \sim \frac{3^{\frac{1}{3}}}{\bar{d}\,\delta^{\frac{1}{2}}}$$

where $Ca = \delta^{\frac{3}{2}}$ and $d \sim \delta\,\bar{d}$. This leading order term checks with the singular perturbation result in section 2.2. This relationship between k, d, and Ca will be compared with the numerical solution.

III. The Use of a Composite Mesh to Solve the Fingering Problem

3.1 Grid Construction

In solving the partial differential equations (2a,b,c), it is important to develop numerical methods that not only give accurate results in the interior of the region, but also give accurate results at the boundaries. To solve the normal-stress boundary condition (6c), it is necessary to compute the pressure and the stresses accurately on the boundary. To accomplish this, we use a composite mesh to cover the domain. This is composed of a rectilinear grid which is parallel to the straight boundaries, and a curvilinear grid which follows the curved interface.

Kreiss [5] has developed a numerical code that constructs a curvilinear grid using spline interpolation that follows the smooth boundary of a simply connected domain. The rest of the domain was covered with a uniformly spaced rectilinear grid. A hyperbolic system was solved on these overlapping grids. Reyna [9] has used a composite mesh to solve an ocean circulation model in a circular basin. A grid using polar coordinates was used on the boundary and a uniformly spaced rectilinear grid was used in the interior. We have modified and improved these methods to best solve the penetration of a finger into a viscous fluid.

To solve the fingering problem numerically, we restrict the infinite domain given by $-\infty < x < \infty$ and $0 \leq y \leq 1$ to a finite domain given by $x_{\min} \leq x \leq x_{\max}$ and $0 \leq y \leq 1$. If the values of $x_{\min}$ and $x_{\max}$ have been chosen properly, the difference between the numerical solution calculated on this domain and the

solution calculated on an even larger domain will be small. As stated in section 2.1, the domain is further restricted to the region exterior to the finger.

In many problems, it is important to distribute the grid points in a nonuniform way to properly resolve the solution. In the fingering problem, a smaller mesh size is needed near $y = 1$ where the fluid moves into the narrow region between the finger and the wall. The grid points are conveniently distributed in the rectilinear grid to place a smaller mesh size where it is needed.

We begin with a square grid with uniformly distributed grid points given by $(\hat{x}_i,\hat{y}_j) = \left(\frac{i-1}{N_x-1}, \frac{j-1}{N_y-1}\right)$, where $i = 1,2,\cdots N_x$ and $j = 1,2,\cdots N_y$. N_x and N_y are the number of grid points in the $\hat{x}$ and $\hat{y}$ directions respectively. The rectilinear grid is defined by a transformation T_r

$$\hat{x} = f(x) \qquad \hat{y} = g(y) \tag{27}$$

which maps the square grid with uniformly distributed grid points onto the domain. An example of a stretched rectilinear grid is shown in Figure 3. The functions f and g used in the fingering problem are given in section 3.3.

To construct the curvilinear grid, we start with another square grid with uniformly distributed grid points given by $(\hat{s}_i,\hat{r}_j) = \left(\frac{i-1}{N-1}, \frac{j-1}{M-1}\right)$, where $i = 1,2,\cdots N$ and $j = 1,2,\cdots M$. There are N grid points in the $\hat{s}$ direction and M grid points in the $\hat{r}$ direction. The curvilinear grid is defined by mapping this square grid onto a region which follows the curved interface using the transformation T_c. This transformation is one-to-one and its Jacobian is never singular. To construct the transformation T_c, a set of N grid points is chosen along the interface. Cubic spline interpolation is used to approximate the shape of the curved interface through these grid points. The boundary $\hat{r} = 0$ of the square

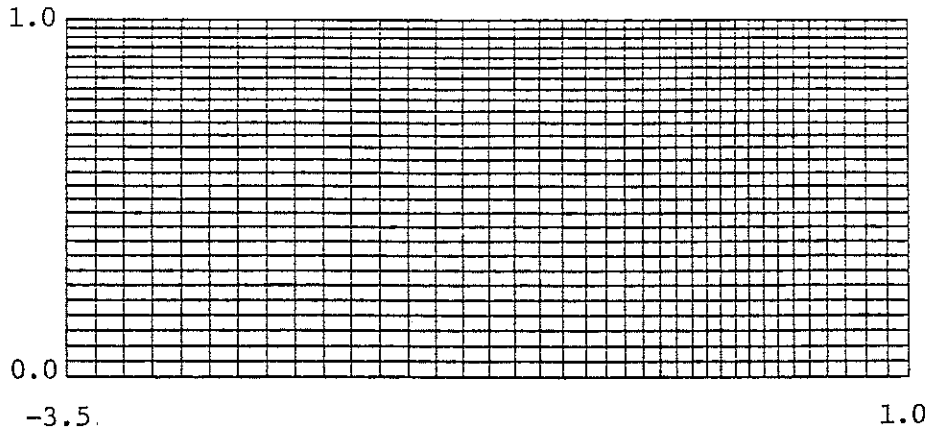

Figure 3

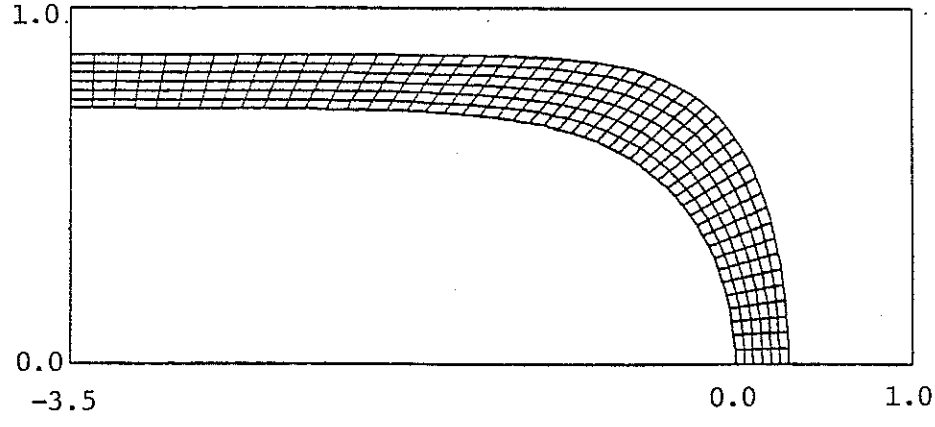

Figure 4

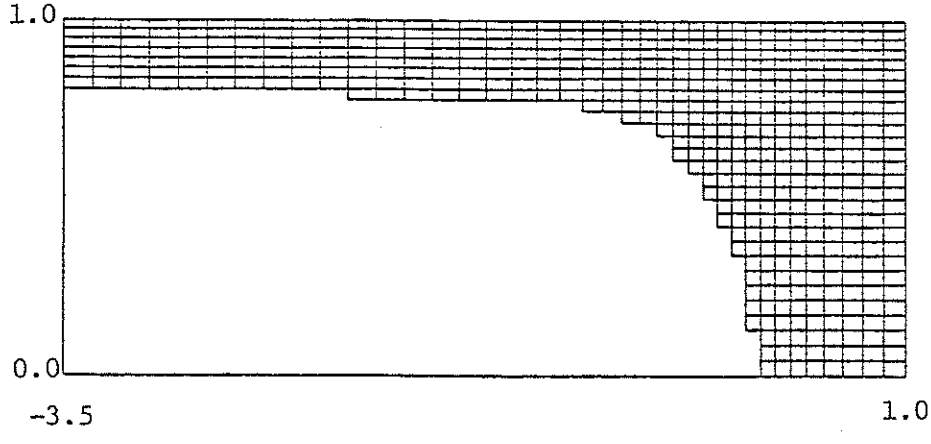

Figure 5

grid is mapped onto the interface curve C_1 by

$$x(\hat{s},0) = X_1(\hat{s}) \qquad y(\hat{s},0) = Y_1(\hat{s})$$

where X_1 and Y_1 are cubic spline functions. Another set of N points is chosen on a curve that lies in the interior of the domain under consideration. The transformation of the boundary $\hat{r} = 1$ onto the interior curve C_M is also done by cubic spline interpolation and given by

$$x(\hat{s},1) = X_M(\hat{s}) \qquad y(\hat{s},1) = Y_M(\hat{s})$$

The curves, C_1 and C_M, form the two curved boundaries of the curvilinear grid. The corresponding grid points on these two curves are connected by straight lines. The complete transformation T_c is

$$\begin{aligned} x(\hat{s},\hat{r}) &= (1-\hat{r})\,X_1(\hat{s}) + \hat{r}\,X_M(\hat{s}) \\ y(\hat{s},\hat{r}) &= (1-\hat{r})\,Y_1(\hat{s}) + \hat{r}\,Y_M(\hat{s}) \end{aligned} \tag{28}$$

To simply the interface condition (6c), it is convenient to use the arclength parameter s along the interface. As in the rectilinear grid, stretching is used in the curvilinear grid to place more grid points at the tip of the finger and fewer grid points where the width of the finger approaches a constant. Stretching is introduced by the transformations

$$\hat{s} = F(s) \qquad \hat{r} = G(r)$$

where F and G are functions that produce a one-to-one mapping between the two sets of variables. The transformation T_c that allows for stretching in the curvilinear grid is

$$\begin{aligned} x(s,r) &= (1-r)\,X_1(s) + r\,X_M(s) \\ y(s,r) &= (1-r)\,Y_1(s) + r\,Y_M(s) \end{aligned} \tag{29}$$

with,

$$s = F^{-1}(\hat{s}) \qquad r = G^{-1}(\hat{r}) \tag{30}$$

where the cubic spline functions are functions of the variable s. The function G is chosen such that $G(1) = 1$. A typical curvilinear grid is shown in Figure 4.

Many of the grid points shown in Figure 3 are in the interior of the finger. These points are not used in the computation of the solution. Figure 5 gives an example of a rectilinear grid that shows only the grid points actually used. It is important that the grids overlap so that all grid points on C_M lie in the interior of the rectilinear grid. Also, the grid points on the jagged boundary of the rectilinear grid must lie in the interior of the curvilinear grid.

3.2 Interpolation Between Grids

In solving partial differential equations on a composite mesh, the grid points can be divided into three categories. At interior points of each grid, difference equations that approximate the partial differential equations are applied. At grid points that lie on the boundary of the domain, boundary conditions are applied. The third type of grid points are those that lie on the interior curve C_M of the curvilinear grid and those that lie on the jagged boundary of the rectilinear grid. It is at these grid points that interpolation equations are used to connect the solutions on the two grids. The interpolation equations are discussed in terms of a smooth function u.

Kreiss [5] finds the approximate value of u at a grid point on the jagged boundary of a rectilinear grid by a four point interpolation formula that uses the value of u at the four closest grid points in the curvilinear grid. A nine point interpolation formula determines the approximate value of u at a grid point in the curvilinear grid by using the value of u at the nine closest points in a uniformly spaced rectilinear grid. In the first case, it was necessary to search four adjacent quadrilaterals to find the one in which the rectilinear boundary point was located and then use an interpolation formula using the values of u at the corners of the quadrilateral. A nine point interpolation formula using the values of u at the corners of the four adjacent quadrilaterals would be more accurate, but would also be quite complicated. In the second case, a different nine point formula must be used if the rectilinear grid is not uniform, as is the case when stretching is used. To avoid these problems, we use interpolation formulas based on the uniformly distributed grid points of the two square grids discussed in section 3.1.

Each grid point on the curve C_M, given by $(s_i,1)$, can be located in the interior of the $(\hat{x},\hat{y})$ square grid by using equations (29) and (27). If $(\hat{x}_0,\hat{y}_0)$ is the location of one of these grid points, then the approximate value of u at this grid point can be found by using the four point interpolation formula

$$u(\hat{x}_0,\hat{y}_0) = \sum_{i=1}^{2}\sum_{j=1}^{2} c_i(\alpha)\, c_j(\beta)\, u(\hat{x}_{I+i-1},\hat{y}_{J+j-1}) \tag{31}$$

$$c_1(\alpha) = 1-\alpha \qquad c_2(\alpha) = \alpha$$

$$\alpha = \frac{\hat{x}_0-\hat{x}_I}{\hat{x}_{I+1}-\hat{x}_I} \qquad \beta = \frac{\hat{y}_0-\hat{y}_J}{\hat{y}_{J+1}-\hat{y}_J}$$

where $(\hat{x}_I,\hat{y}_J)$ is the lower left corner of the rectangle in which the point $(\hat{x}_0,\hat{y}_0)$ is located. A nine point interpolation formula is given by

$$u(\hat{x}_0,\hat{y}_0) = \sum_{i=1}^{3}\sum_{j=1}^{3} d_i(\alpha)\, d_j(\beta)\, u(\hat{x}_{I+i-2},\hat{y}_{J+j-2}) \tag{32}$$

$$d_1(\alpha) = -\tfrac{1}{2}\alpha(1-\alpha) \qquad d_2(\alpha) = (1-\alpha)(1+\alpha) \qquad d_3 = \tfrac{1}{2}\alpha(1+\alpha)$$

where $(\hat{x}_I,\hat{y}_J)$ is the grid point closest to the point $(\hat{x}_0,\hat{y}_0)$. The values of α and β are the same as for the four point formula.

To find the approximate value of u at each (x,y) grid point on the jagged boundary, we locate each of these grid points in the interior of the $(\hat{s},\hat{r})$ square grid. These values are found by using Newton's method on equations (29) and (30). Once these points are located, the interpolation formulas are identical with equations (31) and (32) where $\hat{x}$ and $\hat{y}$ are replaced by $\hat{s}$ and $\hat{r}$.

3.3 Test of the Composite Mesh Technique

Saffman and Taylor [13] have derived a close form solution for the penetration of a fluid into a Hele-Shaw cell containing a more viscous liquid. The solution is derived by first averaging the velocity field in the direction between the plates. The equations for the components of the mean velocity, in the plane parallel to the plates, are given by

$$u = -\frac{b^2}{3\mu}\frac{\partial p}{\partial x} \qquad v = -\frac{b^2}{3\mu}\frac{\partial p}{\partial y}$$

where the distance $2b$, between the plates, is much smaller than the width of the cell. Since the fluid is incompressible, the continuity equation given by

$$\frac{\partial u}{\partial x} + \frac{\partial v}{\partial y} = 0$$

must also be satisfied. The components of the mean velocity can be expressed in terms of a velocity potential φ and a stream function ψ

$$u = \frac{\partial \varphi}{\partial x} = \frac{\partial \psi}{\partial y} \qquad v = \frac{\partial \varphi}{\partial y} = -\frac{\partial \psi}{\partial x}$$

The velocity potential and stream function satisfy the Cauchy-Riemann equations; thus, $\omega = \varphi + i\psi$ is an analytic function of $z = x + iy$. The closed form solution satisfying the appropriate boundary conditions is

$$z = \frac{\omega}{\lambda} + \frac{2(1-\lambda)}{\pi} \log \frac{1}{2}\left[1+\exp\left[-\frac{\pi\omega}{\lambda}\right]\right] \tag{33}$$

where ω is given as an implicit function of z. The parameter λ is equal to the (width of the finger)/(width of the channel). The boundary conditions on the interface are $\varphi = 0$ and $\psi = y$. Substitution of these values into equation (33) gives an equation for the free surface

$$x = \frac{2(1-\lambda)}{\pi} \log\left[\cos\frac{\pi y}{2\lambda}\right] \tag{34}$$

Though it was shown by Saffman and Taylor that the difference between the above solution and their experimental results is considerable unless λ is close to $\frac{1}{2}$, their closed form solution is very useful in testing the use of a composite mesh to numerically solve for the stream function ψ. It should also be noted that the Saffman-Taylor solution is for a finger moving in the plane parallel to the plates and not in the narrow region between the two plates, which is the focus of this thesis.

Since ω is an analytic function of z, its real and imaginary parts must satisfy Laplace's equation; thus,

$$\frac{\partial^2 \psi}{\partial x^2} + \frac{\partial^2 \psi}{\partial y^2} = 0 \tag{35}$$

The boundary conditions for ψ are

$$\begin{aligned} \psi(x,0) &= 0 \quad \text{for} \quad 0 \leq x \leq \infty \\ \psi(x,1) &= \lambda \quad \text{for} \quad -\infty \leq x \leq \infty \end{aligned} \tag{36a,b}$$

and on the interface

$$\psi(x,y) = y \tag{36c}$$

where the shape of the interface is given by equation (34). The asymptotic behavior of ψ as $x \to -\infty$ is

$$\psi(x,y) \to \lambda \tag{36d}$$

and the behavior as $x \to \infty$ is

$$\psi(x,y) \to \lambda y \tag{36e}$$

These asymptotic behaviors are used as boundary conditions at some finite $x_{\min}$ and $x_{\max}$.

The resulting problem is to solve Laplace's equation on a domain with an irregular shape, where the value of ψ is given on the boundary. To solve the problem numerically, equation (35) is replaced by difference equations at the uniformly distributed grid points of the two square grids. These grids are related to the rectilinear and curvilinear grids through the transformations T_r and T_c.

We write equation (35) in terms of $\hat{x}$ and $\hat{y}$ coordinates by using equation (27).

$$f'(x)\frac{\partial}{\partial \hat{x}}\left[f'(x)\frac{\partial \psi}{\partial \hat{x}}\right] + g'(y)\frac{\partial}{\partial \hat{y}}\left[g'(y)\frac{\partial \psi}{\partial \hat{y}}\right] = 0 \tag{37}$$

where

$$x = f^{-1}(\hat{x}) \qquad y = g^{-1}(\hat{y})$$

As previously discussed, stretching functions f and g are introduced to avoid placing extra grid points where they are not needed. In the x direction, fewer grid points are needed near $x_{\min}$ and $x_{\max}$ where the solution tends to a function of y only. The x dependence is a decaying exponential. The stretching is accomplished by using a mesh size h_o near the boundaries and a smaller mesh size h_i in an interior region centered about the point x_0. The function f takes the form,

$$\hat{x} = f(x) = A\,x + B + C \cdot E \tanh\left(\frac{x - x_0}{E}\right) \tag{38}$$

where the first derivative is given by

$$\frac{d\hat{x}}{dx} = f'(x) = A + C\ \mathrm{sech}^2\left(\frac{x - x_0}{E}\right) \tag{39}$$

The constant B is chosen such that $f(x_{\min}) = 0$. The other constants are given by

$$A = \frac{\bar{h}_x}{h_o} \qquad C = \frac{\bar{h}_x}{h_i} - \frac{\bar{h}_x}{h_o} \qquad E = \left(\frac{h_i}{h_o}\right)^{\frac{1}{2}}$$

where $\bar{h}_x$ is chosen such that $f(x_{\max}) = 1$. The number of grid points and the mesh size in the $\hat{x}$ direction of the square grid are

$$N_x = \text{integer}\left(\frac{1}{\bar{h}_x} + 1.5\right) \qquad h_x = \frac{1}{N_x - 1}$$

where h_x is approximately equal to $\bar{h}_x$. An examination of (39) shows that $\frac{d\hat{x}}{dx}$ is approximately equal to $\frac{h_x}{h_i}$ when x is near x_0. It also shows that $\frac{d\hat{x}}{dx}$ is approximately equal to $\frac{h_x}{h_o}$ when x is near the boundaries. Notice also that if we set $h_i = h_o$, then equation (38) is a linear transformation and no stretching is done.

In the perturbation problem, it was found that for Ca small the finger nearly fills the channel. To numerically solve the fingering problem for Ca small, it is necessary to have a small mesh size near $y = 1$. To avoid a small mesh size in the entire y direction, we use a mesh size h_b away from $y = 1$ and a smaller mesh size h_t near $y = 1$. The stretching in the y direction takes the form

$$\hat{y} = g(y) = A\,y + C\cdot E\left[\exp\left(\frac{-(1-y)}{E}\right) - \exp\left(\frac{-(1+y)}{E}\right)\right] \tag{40}$$

where the first derivative is given by

$$\frac{d\hat{y}}{dy} = g'(y) = A + C\left[\exp\left(\frac{-(1-y)}{E}\right) + \exp\left(\frac{-(1+y)}{E}\right)\right] \tag{41}$$

The constants are given by

$$A = \frac{\bar{h}_y}{h_b} \qquad C = \frac{\bar{h}_y}{h_t} - \frac{\bar{h}_y}{h_b} \qquad E = \frac{h_t}{h_b}$$

where $\bar{h}_y$ is chosen such that $g(1) = 1$. The number of grid points and the mesh size in the $\hat{y}$ direction of the square grid are

$$N_y = \text{integer}\left(\frac{1}{\bar{h}_y} + 1.5\right) \qquad h_y = \frac{1}{N_y - 1}$$

where h_y is approximately equal to $\bar{h}_y$. An examination of equation (41) shows

that $\frac{d\hat{y}}{dy}$ is approximately equal to $\frac{h_y}{h_t}$ when y is close to 1, and $\frac{d\hat{y}}{dy}$ is approximately equal to $\frac{h_y}{h_b}$ for y away from 1. As before, if we set $h_t = h_b$, then equation (40) is a linear transformation and no stretching is done.

Using the notation $\psi_{i,j} = \psi(\hat{x}_i, \hat{y}_j)$, a second order difference equation for equation (37) is given by

$$\begin{aligned} &\frac{f'_i}{h_x}\left[f'_{i+\frac{1}{2}}\left(\frac{\psi_{i+1,j}-\psi_{i,j}}{h_x}\right) - f'_{i-\frac{1}{2}}\left(\frac{\psi_{i,j}-\psi_{i-1,j}}{h_x}\right)\right] \\ &+ \frac{g'_j}{h_y}\left[g'_{j+\frac{1}{2}}\left(\frac{\psi_{i,j+1}-\psi_{i,j}}{h_y}\right) - g'_{j-\frac{1}{2}}\left(\frac{\psi_{i,j}-\psi_{i,j-1}}{h_y}\right)\right] = 0 \end{aligned} \tag{42}$$

where we define the expression $f'_{i+\frac{1}{2}}$ by

$$f'_{i+\frac{1}{2}} = \frac{1}{2}\left[f'(x_i) + f'(x_{i+1})\right]$$

This difference equation is used at all interior grid points of the $(\hat{x}, \hat{y})$ square grid.

A second order difference equation for equation (35) at the uniformly distributed grid points of the $(\hat{s}, \hat{r})$ square grid is found by using equations (29) and (30). If we first define

$$\begin{aligned} a(s,r) &= F''(s)\frac{\partial s}{\partial x} \qquad & b(s,r) &= F''(s)\frac{\partial s}{\partial y} \\ c(s,r) &= G'(r)\frac{\partial r}{\partial x} \qquad & d(s,r) &= G'(r)\frac{\partial r}{\partial y} \end{aligned} \tag{43}$$

then equation (35) becomes

$$\begin{aligned} &a\frac{\partial}{\partial \hat{s}}\left[a\frac{\partial \psi}{\partial \hat{s}} + c\frac{\partial \psi}{\partial \hat{r}}\right] + c\frac{\partial}{\partial \hat{r}}\left[a\frac{\partial \psi}{\partial \hat{s}} + c\frac{\partial \psi}{\partial \hat{r}}\right] \\ &+ b\frac{\partial}{\partial \hat{s}}\left[b\frac{\partial \psi}{\partial \hat{s}} + d\frac{\partial \psi}{\partial \hat{r}}\right] + d\frac{\partial}{\partial \hat{r}}\left[b\frac{\partial \psi}{\partial \hat{s}} + d\frac{\partial \psi}{\partial \hat{r}}\right] = 0 \end{aligned} \tag{44}$$

The partial derivatives in equation (43) are calculated at each grid point by first calculating $\frac{\partial x}{\partial s}$, $\frac{\partial y}{\partial s}$, $\frac{\partial x}{\partial r}$, and $\frac{\partial y}{\partial r}$ from equation (29). The first derivatives of X_1, X_M, Y_1, and Y_M at the grid points are already known from cubic spline interpolation. The formulas connecting the two sets of partial derivatives are

$$\frac{\partial s}{\partial x} = \frac{\frac{\partial y}{\partial r}}{\Delta} \qquad \frac{\partial s}{\partial y} = -\frac{\frac{\partial x}{\partial r}}{\Delta} \qquad \frac{\partial r}{\partial x} = -\frac{\frac{\partial y}{\partial s}}{\Delta} \qquad \frac{\partial r}{\partial y} = \frac{\frac{\partial x}{\partial s}}{\Delta}$$

$$\Delta = \frac{\partial x}{\partial s}\frac{\partial y}{\partial r} - \frac{\partial x}{\partial r}\frac{\partial y}{\partial s}$$

In the s direction, we use a stretching transformation that produces more grid points in the region near the tip of the finger. The transformation is given by

$$\hat{s} = F(s) = \frac{h_s}{h_N}\left[s + (R-1)\,D\tanh\left[\frac{s}{D}\right]\right] \tag{45}$$

where the derivative is

$$\frac{d\,\hat{s}}{d\,s} = F'(s) = \frac{h_s}{h_N}\left[1 + (R-1)\,\mathrm{sech}^2\left[\frac{s}{D}\right]\right] \tag{46}$$

The input parameters used to specify the transformation are N, the number of grid points, R, the ratio between the largest and smallest mesh size, D, the decay rate from one mesh size to the other, and s_{max}, the largest value of s used in the grid. The constant h_s is the mesh size in the $\hat{s}$ direction of the square grid and is given by $h_s = \frac{1}{N-1}$. The largest mesh size h_N is determined by satisfying $F(s_{max}) = 1$. The smallest mesh size h_1 is $h_1 = \frac{h_N}{R}$.

On the free surface, there is no boundary layer to resolve by stretching. The function $G(r)$ is given by $\hat{r} = G(r) = r$ where the mesh size in the $\hat{r}$ direction is $h_r = \frac{1}{M-1}$.

If we define $\psi_{i,j} = \psi(s_i, r_j)$ and $a_{i,j} = a(s_i, r_j)$, then second order difference formulas for typical terms in equation (44) are

$$a \frac{\partial}{\partial \hat{s}} \left[a \frac{\partial \psi}{\partial \hat{s}} \right] = \frac{a_{i,j}}{h_s} \left[a_{i+\frac{1}{2},j} \left[\frac{\psi_{i+1,j} - \psi_{i,j}}{h_s} \right] - a_{i-\frac{1}{2},j} \left[\frac{\psi_{i,j} - \psi_{i-1,j}}{h_s} \right] \right]$$

and

$$c \frac{\partial}{\partial \hat{r}} \left[a \frac{\partial \psi}{\partial \hat{s}} \right] = \frac{c_{i,j}}{h_r} \left[a_{i,j+1} \left[\frac{\psi_{i+1,j+1} - \psi_{i-1,j+1}}{h_s} \right] - a_{i,j-1} \left[\frac{\psi_{i+1,j-1} - \psi_{i-1,j-1}}{h_s} \right] \right]$$

The expression $a_{i+\frac{1}{2},j}$ is defined by

$$a_{i+\frac{1}{2},j} = \frac{1}{2} \left[a_{i,j} + a_{i+1,j} \right]$$

The second order difference equation for equation (44) is applied at all interior points of the $(\hat{s}, \hat{r})$ square grid.

The numerical solution for ψ in equation (35) can be found by using these difference equations, the interpolation equations from section 3.2, and the boundary conditions (36). We compare the numerical solution with the closed form solution for λ = 0.5, 0.6, 0.7, 0.8, and 0.9. The mesh sizes and number of grid points used for the curvilinear grid are given in table 1. The error e_{sr} is the maximum error at any grid point in the curvilinear grid. Table 2 gives the data used for the rectilinear grid for each value of λ. The maximum error at any grid point in the rectilinear grid is e_{xy}. Both four and nine point interpolation formulas worked equally well in this problem. The nine point formula was used to

determine the data in tables 1 and 2.

As an alternative to simply setting ψ equal to its asymptotic value at $x = x_{max}$, the boundary condition

$$\frac{\partial \psi}{\partial x} + \pi\left(\psi - \lambda y\right) = 0$$

was applied at $x = x_{max}$. This boundary condition allows the first eigenfunction with the slowest decay rate as $x \to \infty$ to be present in the solution at $x = x_{max}$. The error in the numerical solution showed some improvement very near $x = x_{max}$ when using the improved boundary condition. In the fingering problem, the eigenfunctions decay exponentially as $x \to \pm \infty$; thus, it was deemed unnecessary to use an improved boundary condition.

Curvilinear Grid

λ	N	h_1	h_N	s_{max}	M	e_{sr}
0.5	51	.04	.08	3.0	7	1.9E-04
0.6	51	.035	.07	2.5	7	1.2E-04
0.7	51	.05	.05	2.5	7	1.1E-04
0.8	51	.04	.04	2.0	7	1.3E-04
0.9	51	.03	.03	1.5	7	5.6E-05

Table 1

Rectilinear Grid

λ	N_x	h_i	h_0	x_{min}	x_{max}	N_y	h_b	h_t	e_{xy}
0.5	45	.07	.14	-2.8	2.0	25	.05	.04	2.2E-04
0.6	41	.07	.14	-2.2	2.0	25	.05	.04	1.6E-04
0.7	40	.07	.14	-2.1	2.0	29	.05	.03	1.6E-04
0.8	49	.05	.10	-1.4	2.0	33	.05	.02	1.4E-04
0.9	53	.03	.10	-0.8	2.0	37	.05	.01	9.3E-05

Table 2

IV. Numerical Solution of the Two-dimensional Problem

4.1 Stream Function and Vorticity Formulation

In solving the fingering problem numerically, it is convenient to express the equations in terms of the stream function and the vorticity. We substitute the stream function ψ

$$u = \psi_y \qquad v = -\psi_x$$

and the vorticity w defined by

$$w = u_y - v_x$$

into equations (2a,b,c). If the pressure is eliminated from the equations, we obtain

$$\begin{aligned} \psi_{xx} + \psi_{yy} &= w \\ w_{xx} + w_{yy} &= 0 \end{aligned} \qquad \text{(48a,b)}$$

On the interface, it is convenient to use an arc-length coordinate s equal to 0 at the origin and increasing along the curved interface. Using the arc-length coordinate, the tangent vector $\mathbf{t}$ is equal to $(x_s(s,0), y_s(s,0))$, and the normal vector $\mathbf{n}$, pointing into the finger, is equal to $(-y_s(s,0), x_s(s,0))$. These values are determined from equation (29). The interface conditions (5a,b,c) become

$$x_s \psi_x + y_s \psi_y = 0$$

$$(y_s^2 - x_s^2)(\psi_{yy} - \psi_{xx}) + 4 x_s y_s \psi_{xy} = 0$$

$$p - 2\,Ca\left[(y_s^2 - x_s^2)\,\psi_{xy} - x_s\,y_s\,(\psi_{yy} - \psi_{xx})\right] = -\frac{1}{R}$$

where Ca equals $\mu U/T$ and

$$\frac{1}{R} = x_s\,y_{ss} - y_s\,x_{ss}$$

These three interface conditions can be rewritten as

$$\psi = 0$$

$$w + 2\,x_{ss}\,\psi_x + 2\,y_{ss}\,\psi_y = 0 \qquad \text{(49a,b,c)}$$

$$p - 2\,Ca\left[(y_s^2 - x_s^2)\,\psi_{xy} - x_s\,y_s\,(\psi_{yy} - \psi_{xx})\right] + x_s\,y_{ss} - y_s\,x_{ss} = 0$$

The symmetry conditions for $x \geq 0$ are

$$\psi(x,0) = 0 \qquad w(x,0) = 0 \qquad \text{(50a,b)}$$

and the boundary conditons on the wall are

$$\psi(x,1) = -(1-\beta) \qquad \psi_y(x,1) = -1 \qquad \text{(51a,b)}$$

The asymptotic behavior of the fluid flow as $x \to -\infty$ is

$$\psi \to -y + \beta \qquad w \to 0 \qquad \text{(52a,b)}$$

and the behavior as $x \to \infty$ is

$$\psi \to \frac{3}{2}\beta\left[y - \frac{1}{3}y^3\right] - y \qquad w \to -3\beta y \qquad \text{(53a,b)}$$

To solve this problem numerically, we begin with an initial guess for the correct shape of the finger. The initial guess is found by starting with a small value for the parameter $Ca = \mu U/T$ and using the perturbation solution. Since the shape of the finger has been fixed, we are forced to drop one of the three

interface conditions (49a,b,c). The normal-stress boundary condition (49c) is dropped. This condition will be used to find the correct shape of the finger.

4.2 Numerical Solution on the Fixed Domain

The system of equations given in section 4.1 is solved in the same way as the equation for ψ in section 3.3 was solved. A curvilinear grid is constructed that follows the curved interface of the finger, and a rectilinear grid is constructed parallel to the straight boundaries. These grids are related to the two square grids with uniformly distributed grid points through the transformations T_c and T_r given in section 3.1. The same second order finite difference methods used in the square grids in section 3.3 are used for equations (48a,b), except for the addition of w on the right-hand side of equation (48a).

The computational boundary conditions for the two-dimensional fingering problem discussed in section 4.1 must be chosen carefully. We consider the boundary conditions at $y = 1$, where, for simplicity, the case with no stretching is examined ($h_b = h_t$). A common method for applying the boundary conditions (51a,b) is to construct a grid where the boundary $y = 1$ is centered between the top two grid lines. This allows us to give the value of ψ on the top two grid lines

$$\psi_{i,N_y} = \psi\left(x_i, 1 + \frac{h_y}{2}\right) = \psi(x_i,1) + \frac{h_y}{2}\psi_y(x_i,1)$$

$$\psi_{i,N_y-1} = \psi\left(x_i, 1 - \frac{h_y}{2}\right) = \psi(x_i,1) - \frac{h_y}{2}\psi_y(x_i,1)$$

where h_y is the mesh size in the y direction. The error in applying these two

boundary conditions is $O(h_y^2 \psi_{yy}(x_i,1))$. If the value of ψ is now given at $x = x_{max}$, then the discontinuity in the value of ψ is $O(h_y^2)$ at the corner $x = x_{max}$ and $y = 1$. It was found that this leads to an $O(1)$ error in the vorticity near the corner. This can be predicted by examining the difference equations for equation (48a). A more detailed explanation of the problems associated with these boundary conditions and an examination of a model problem can be found in the appendix. If the boundary is a simple smooth curve, then these computational boundary conditions can be used and no discontinuity will develop. Also, if the value of $\psi_{yy}(x_i,1)$ equals zero at the corner, then the discontinuity in the value of ψ is not $O(h_y^2)$ and the vorticity error is $o(1)$. The driven cavity problem is an example of this last case. Unfortunately, the value of $\psi_{yy}(x_{max},1)$ is not equal to zero in our problem; thus, the computational boundary conditions discussed above should not be used.

We constuct the rectilinear grid with the top grid line coincident with the boundary $y = 1$. The boundary condition (51a) gives the value of ψ on the top grid line. A second order boundary condition for the vorticity w at $y = 1$ is derived by using the values of ψ on the top three grid lines and the value of ψ_y at $y = 1$. This boundary condition is given by

$$w_{i,N_y} = \frac{-7\psi_{i,N_y} + 8\psi_{i,N_y-1} - \psi_{i,N_y-2}}{2h_y^2} + \frac{3\psi_y(x_i,1)}{h_y}$$

where h_y is the mesh size in the y direction. To use stretching, the boundary conditions are transformed to the square grid, and similar difference equations are applied.

On the interface, the curvilinear grid is constructed with the grid line ($\hat{r} = 0$) coincident with the shape of the interface curve. The boundary conditions applied on the interface are written in terms of s and r coordinates by

$$\psi = 0$$

$$w + 2\left[x_{ss}\, r_x + y_{ss}\, r_y\right]\psi_r = 0$$

ψ_s is equal to zero on the interface. The value of ψ_r is calculated to second order by using the first three grid lines in the r direction.

As discussed in section 3.3, the asymptotic behaviors of ψ and w as $x \to \pm\infty$ are applied at $x = x_{max}$ and $x = x_{min}$. The value of x_{min} is decreased and the value of x_{max} is increased to verify that the shape of the interface curve does not change. An examination of the contour plots shows that the contour lines flatten out rapidly away from the tip of the finger; thus, the size of the domain need not be excessively large.

4.3 Calculation of the Pressure and the Stresses on the Curved Interface

To determine the degree to which the normal-stress boundary conditon is satisfied, it is necessary to find the pressure and the stresses on the interface. The pressure is calculated from the vorticity solution by integrating along the interface. The pressure is given in terms of the vorticity by

$$p_x = Ca\, w_y \qquad p_y = -Ca\, w_x$$

Using the transformation T_c and these relationships between the pressure and the vorticity, the derivative of the pressure with respect to arc length is

$$p_s = x_s\, p_x + y_s\, p_y$$

$$= Ca\left[x_s\, w_y - y_s\, w_x\right]$$

$$= Ca\, x_s\left[s_y w_s + r_y w_r\right] - Ca\, y_s\left[s_x w_s + r_x w_r\right]$$

$$= Ca\left[x_s r_y - y_s r_x\right] w_r + Ca\left[x_s s_y - y_s s_x\right] w_s$$

If we define

$$A(s,r) = \frac{Ca\, G'(r)}{F'(s)}\left[x_s r_y - y_s r_x\right] \qquad B(s,r) = \mathrm{Ca}\left[x_s s_y - y_s s_x\right]$$

then the pressure equation written in $\hat{s}$ and $\hat{r}$ coordinates is

$$p_{\hat{s}} = A(s,r)\, w_{\hat{r}} + B(s,r)\, w_{\hat{s}}$$

An explicit second order difference equation for the pressure is

$$p_{i,1} = p_{i+1,1} - h_s A_{i+\frac{1}{2},1}\left[\frac{-3w_{i+\frac{1}{2},1} + 4w_{i+\frac{1}{2},2} - w_{i+\frac{1}{2},3}}{2h_r}\right] - B_{i+\frac{1}{2},1}\left[w_{i+1,1} - w_{i,1}\right]$$

where expressions like $A_{i+\frac{1}{2},1}$ are defined by

$$A_{i+\frac{1}{2},1} = \frac{1}{2}\left[A(s_i, r_1) + A(s_{i+1}, r_1)\right]$$

as in section 3.3. The value of $p_{N,1}$, the value of the pressure in the region where the finger flattens out, is set equal to the constant pressure in the interior of the finger, which has been set equal to zero.

The stresses ψ_{xx}, ψ_{xy}, and ψ_{yy} are calculated at each grid point on the curved interface from the matrix equation

$$\begin{bmatrix} 1 & 0 & 1 \\ x_s^2 & 2x_s y_s & y_s^2 \\ x_s x_r & x_s y_r + x_r y_s & y_s y_r \end{bmatrix} \begin{bmatrix} \psi_{xx} \\ \psi_{xy} \\ \psi_{yy} \end{bmatrix} = \begin{bmatrix} w \\ \frac{1}{2}w \\ \psi_{sr} - (x_{sr} r_x + y_{sr} r_y)\psi_r \end{bmatrix}$$

The second and third equations are expressions for ψ_{ss} and ψ_{sr}. They have been simplified by using the interface conditions (49a,b). The values of ψ_r and ψ_{sr} are calculated to second order on the interface by using the first three grid lines in the r direction. The derivatives x_{rs} and y_{rs} of the transformation T_c are determined from equation (29).

We substitute the initial guess for the shape of the interface and the values of the pressure and stresses at each grid point on the interface into the normal-stress boundary condition (49c). If this boundary condition is satisfied, we have found the correct shape of the finger. Normally, the right-hand side of the normal-stress boundary condition is not equal to zero at each grid point, but a residual R_i is present. If the residuals R_i, $i = 1,2, \cdots N$, are all smaller than a chosen error tolerance, then the correct shape of the interface has been found.

4.4 Expansion of the Interface in Terms of Tchebycheff Polynomials

To change the shape of the interface, it is convenient to expand the interface in terms of a set of functions and unknown parameters. The shape of the finger is determined by the numerical values of these parameters. The form of the expansion greatly effects the amount of computing time needed to converge to the correct interface shape that satisfies the normal-stress boundary condition. In fact, if the expansion is not chosen properly, the problem may never converge.

The interface could be expanded in terms of cubic spline functions and the coordinate values at the grid points on the interface. The residual at each grid

point would be a function of these coordinate values

$$R_i(x_1, y_1, x_2, y_2, \cdots x_N, y_N) \tag{54}$$

The advantage of using cubic spline interpolation is that part of the construction of the transformation T_c would already have been done. One disadvantage is that there are $2N$ parameters in equation (60); thus, calculation of the Jacobian needed in the iteration method would be very time consuming. A furthur disadvantage is that a small perturbation added to a coordinate value has a local effect on the shape of the curve. The iteration method using these local effects is unsatisfactory.

In order to avoid these problems, the interface is expanded in such a way that a perturbation of each parameter produces a global change in the shape of the finger. This allows for the use of fewer parameters which will reduce the computation time. One possible expansion of the interface would be in terms of the arclength s

$$x(s) = \sum_{j=0}^{m} c_j f_j(s)$$

$$y(s) = \sum_{j=0}^{m} d_j g_j(s)$$

where it is necessary to satisfy the extra condition

$$(x')^2 + (y')^2 = 1$$

Both $f_j(s)$ and $g_j(s)$ are global functions of s. This is a satisfactory representation for the interface, except that it requires choosing the c_j's and d_j's to satisfy both the the normal-stress boundary condition and the extra condition.

To avoid introducing extra conditions, the interface is expanded as a function of y. The expansion for the shape of the finger is given by

$$x(y) = \frac{1}{k} \log \left\{ \left[1 - \left(\frac{y}{\beta} \right)^2 \right] \left[1 + \left(\frac{y}{\beta} \right)^2 \sum_{j=0}^{m} c_j \, T_{2j} \left(\frac{y}{\beta} \right) \right] \right\} \tag{55}$$

where $\beta, k, c_0, c_1, \cdots c_m$ are the parameters that determine the shape of the interface. The expansion is constructed so that the tip of the finger is located at the origin and $x(-y)$ is equal to $x(y)$. The functions T_{2j} are the even Tchebycheff polynomials. If the grid points on the interface are projected onto the y-axis, there are many more points near the ends of the interval, $-\beta \leq y \leq \beta$, than near the center of the interval. This is characteristic of the so-called Tchebycheff abiscissae. The Tchebycheff polynomials are chosen because it is expected that they will converge rapidly given the distribution of grid points used in the fingering problem. This is indeed found to be the case.

The asymptotic behavior of the shape of the finger as $x \to -\infty$ is

$$y \sim \beta - A \exp(kx)$$

This relationship is inverted to give

$$x \sim \frac{1}{k} \log \left[\frac{\beta}{A} \left(1 - \frac{y}{\beta} \right) \right]$$

as $y \to \beta$. The expansion is constructed so that this asymptotic behavior is included. If this is a good expansion, the value of c_j will decrease as j increases. This allows us to use the finite series from $j = 1$ to m as a good approximation to the infinite series.

4.5 Iteration Method Used to Determine Shape of the Interface

For a given value of $Ca = \mu U/T$, the correct shape for the interface is determined when we calculate β, k, c_0, c_1, $\cdots c_m$ such that the residual of the normal-stress boundary condition is approximately equal to zero

$$R_i(\beta, k, c_0, c_1, \cdots c_m) \approx 0 \tag{56}$$

for $i = 1, 2, \cdots N$. We use Newton's method to determine the parameters that satisfy this equation. Since the values of the pressure p and the stresses ψ_{xx}, ψ_{xy}, and ψ_{yy} depend on the parameters in some unknown way, there is not a simple functional relationship between R_i and the unknown parameters. In order to calculate the Jacobian of equation (56), a small step size h is added to each parameter independently and the value of R_i is determined. For example, we calculate

$$R_i(\beta+h, k, c_0, c_1, \cdots c_m)$$

which is used to determine the entries of the Jacobian

$$\frac{\partial R_i}{\partial \beta} = \frac{R_i(\beta+h, \cdots) - R_i(\beta, \cdots)}{h}$$

R_i is calculated $m+3$ times, once for each of the parameters. The amount of computing time needed to calculate R_i can be greatly reduced if we do not solve the entire system of equations directly each time.

We begin with an initial shape for the interface defined by a set of parameters and the interface equation (55). We construct the grids and difference equations as previously discussed. This leads to a large sparse system of linear equations for the values of ψ and w at the grid points of the rectilinear and curvilinear grids. If $\mathbf{v}$ is the vector that contains ψ and w, then the system of

linear equations is written

$$\mathbf{A}\,\mathbf{v} = \mathbf{b}$$

To solve this system of linear equations, we determine the **LU** decomposition of the matrix **A**, where **L** is a lower triangular matrix and **U** is an upper triangular matrix. This linear system of equations now decomposes into two triangular systems that are solved by forward substitution and back-substitution. This decomposition of **A** involves a major portion of the computation time.

In order to calculate the value of $R_i(\beta+h, k, c_0, \cdots c_m)$ and the value of the R_i's found by perturbing the other parameters, it is necessary to solve a new system of linear equations

$$\bar{\mathbf{A}}\,\bar{\mathbf{v}} = \bar{\mathbf{b}}$$

Since this new system of equations is a perturbation of the original system of equations, it can be rewritten as

$$(\mathbf{A}+\mathbf{A}_1)\,\bar{\mathbf{v}} = (\mathbf{b}+\mathbf{b}_1)$$

where **A** and **b** are the matrices in the original system. The matrices $\mathbf{A}_1$ and $\mathbf{b}_1$ contain the small perturbations to the original system for small values of h. If we set

$$\bar{\mathbf{v}} = \mathbf{v}+\mathbf{v}_1+\mathbf{v}_2+\mathbf{v}_3+\cdots$$

then the solution to the new system of equations can be determined by solving the following equations:

$$\mathbf{A}\,\mathbf{v}_1 = \mathbf{b}_1 - \mathbf{A}_1\,\mathbf{v}$$

$$\mathbf{A}\,\mathbf{v}_2 = -\mathbf{A}_1\,\mathbf{v}_1$$

$$\mathbf{A}\,\mathbf{v}_3 = -\mathbf{A}_1\,\mathbf{v}_2$$

Since the **LU** decomposition of **A** is known and the right hand side of each of these equations is known from the previous step, these equations are easily solved by forward substitution and back-substitution. In practice, the value of $\bar{\mathbf{v}}$ is determined to six places by solving only two or three of these equations. Using this method, the computation time necessary to compute the Jacobian is essentially equivalent to the time needed to solve the original system.

We use Newton's method to find the new interface curve. The equation is given by

$$\begin{pmatrix} \frac{\partial R_1}{\partial \beta} & \frac{\partial R_1}{\partial k} & \cdots & \frac{\partial R_1}{\partial c_m} \\ \frac{\partial R_2}{\partial \beta} & \frac{\partial R_2}{\partial k} & \cdots & \frac{\partial R_2}{\partial c_m} \\ \vdots & \vdots & & \vdots \\ \vdots & \vdots & & \vdots \\ \frac{\partial R_N}{\partial \beta} & \frac{\partial R_N}{\partial k} & \cdots & \frac{\partial R_N}{\partial c_m} \end{pmatrix} \begin{pmatrix} \delta\beta \\ \delta k \\ \vdots \\ \vdots \\ \delta c_m \end{pmatrix} = \begin{pmatrix} -R_1 \\ -R_2 \\ \vdots \\ \vdots \\ -R_N \end{pmatrix}$$

Since the number of parameters is smaller than the number of grid points on the interface, the least-squares solution to the matrix equation is determined. The new set of parameters is determined by adding $\delta\beta, \delta k, \delta c_0, \cdots \delta c_m$ to the old values of the parameters. This process is repeated until the values of R_i, $i = 1,2, \cdots N$ are smaller than a given error tolerance.

4.6 Numerical Calculations

In order to determine the appropriate interpolation formulas needed to accurately solve equations (48a,b), an exact solution to these equations is examined. The exact solution does not satisfy the boundary conditions used for the fingering problem. Even though the fingering boundary conditions cannot be used for the test problem, we use boundary conditions that have the same form. For example, on the interface we set

$$\psi = f_1(s)$$

$$w + 2\left(x_{ss} r_x + y_{ss} r_y\right)\psi_r = f_2(s)$$

where f_1 and f_2 are chosen such that the exact solution satisfies these two conditions. Three different combinations of interpolation formulas are examined. In case 1, the four point interpolation formula is used for both ψ and w. In case 2, the nine point formula is used for ψ and the four point formula is used for w. Case 3 uses the nine point formula for both ψ and w. We find that the error in ψ and w in cases 2 and 3 is an order of magnitude smaller than the error produced in case 1. Case 3 is used to calculate the data given in Table 3.

Three different rectilinear grids are used to determine the solution. For each grid, stretching in the x-direction remains the same. The values of the parameters used are

$$h_i = 0.08 \qquad h_o = 0.18$$

$x_{max} = 1.0$ and $x_{max} = 2.0$ are used for the right-hand boundary. In both cases, the shape of the finger is the same. The value of x_{min} is determined by the choice of s_{max}; x_{min} is approximately equal to -3.5. The three different sets of

the parameters that determine the stretching in the y-direction are

Mesh 1	$h_b = 0.060$	$h_t = 0.01$
Mesh 2	$h_b = 0.055$	$h_t = 0.02$
Mesh 3	$h_b = 0.050$	$h_t = 0.03$

The mesh with the smallest grid size near $y = 1$ is used when the value of β is close to one. In the s-direction, the mesh size near s_{max} is three times larger than the mesh size near the tip of the finger

$$h_1 = 0.04 \qquad h_N = 0.12$$

where s_{max} is equal to 4.0. The typical number of grid points used in each direction of the curvilinear and rectilinear grids is

$$N = 51 \qquad M = 7 \qquad N_x = 35 \qquad N_y = 30$$

The shape of the finger is determined by using nine parameters ($m = 6$) for the expansion of the interface given in equation (55). The magnitude of the final coefficient c_6 is $O(1.E{-}4)$. The inclusion of a greater number of parameters has very little effect on the shape of the finger.

The numerical results are calculated by beginning with $\mu U/T = 0.01$ and using the known shape of the perturbation solution. Several iterations are needed until the normal-stress boundary condition is satisfied. The value of $\mu U/T$ is then increased by small increments. The shape of the interface at the previous value of $\mu U/T$ is used as the basis for determining the new interface shape at the subsequent value of $\mu U/T$. Three or four iterations are needed for the normal-stress boundary condition to be satisfied at each value of $\mu U/T$. Table 3 gives the values of β, R_0, and Δp at each value of $\mu U/T$ for which the numerical solution is determined. R_0 is the radius of curvature at the tip of the

finger which has been normalized by b, and Δp is the drop in pressure across the tip of the finger which has been normalized by T/b. The value of $R_0 \cdot \Delta p$ is not equal to -1 because of the normal stress contribution.

Finger profiles and contour plots of the stream function and the vorticity are shown in Figures 6, 7, 8, and 9 for the values of $\mu U/T$ equal to 0.04, 0.10, 0.40, and 1.00. As $x \to \infty$, the velocity in the x-direction is

$$u \to \frac{3}{2}\beta(1-y^2)-1$$

When the value of β is greater than $\frac{2}{3}$, the fluid near the x-axis moves with a velocity greater than that of the finger. In this case, an additional stagnation point is present on the interface. For all values of β, there is a stagnation point at the tip of the finger. Both of these stagnation points are seen by examining the contour plots of the stream function. The largest stresses occur where the fluid is forced into the narrow region between the wall and the finger. This is particularly evident when the finger nearly fills the cell.

Figure 10 is a plot of $q = k(1-\beta)$ versus $\mu U/T$. Curve 1 is a plot using the numerical solutions. Curve 2 is a plot of equation (26) which was determined by expanding the solution in terms of eigenfunctions as $x \to -\infty$. The third curve was determined from the perturbation solution. As mentioned in section 2.3, the equation that determines the third curve is equivalent to the leading order behavior of equation (26). An examination of Figure 10 shows that the perturbation solution is valid only for very small values of $\mu U/T$. The plot of $k(1-\beta)$ versus $\mu U/T$ calculated from the numerical solutions is very close to the analytical result plotted in curve 2. The small discrepancy between the two curves is due to the difficulty in calculating the value of k, the exponential decay rate as $x \to -\infty$. Of all the parameters used to determine the shape of the interface, the

value of k is the most sensitive to changes in the grids, while β is the least sensitive. Figures 11, 12, and 13 are plots of β, R_0, and Δp versus $\mu U/T$. To demonstrate the range of validity of the perturbation solution, a plot of β determined by the perturbation solution is also shown.

$\mu U/T$	β	R_0	Δp
0.01	0.946	0.858	-1.15
0.02	0.920	0.795	-1.22
0.04	0.884	0.714	-1.33
0.06	0.860	0.660	-1.43
0.08	0.840	0.620	-1.51
0.10	0.824	0.588	-1.58
0.15	0.794	0.530	-1.74
0.20	0.772	0.491	-1.87
0.25	0.754	0.461	-2.00
0.30	0.740	0.438	-2.12
0.35	0.729	0.419	-2.23
0.40	0.719	0.404	-2.33
0.50	0.703	0.379	-2.53
0.60	0.690	0.361	-2.71
0.70	0.680	0.347	-2.89
0.80	0.672	0.336	-3.06
0.90	0.665	0.326	-3.21
1.00	0.659	0.318	-3.37
1.20	0.649	0.305	-3.67
1.40	0.642	0.296	-3.97
1.60	0.636	0.288	-4.25
1.80	0.631	0.282	-4.53
2.00	0.627	0.277	-4.81
3.00	0.614	0.261	-6.17

Table 3

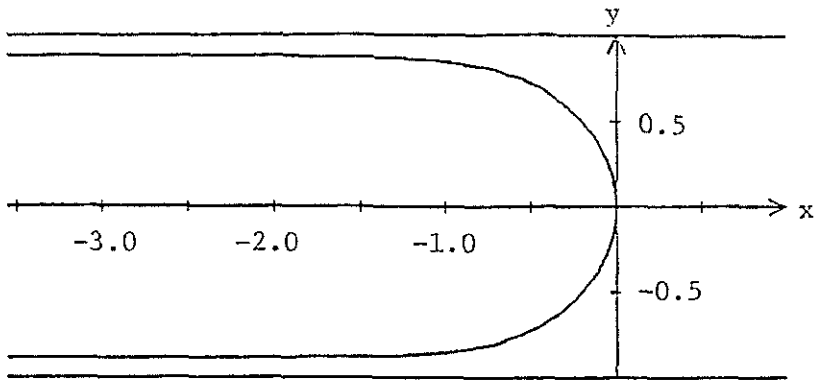

Figure 6a

Two-dimensional Finger Profile $\mu U/T = 0.04$

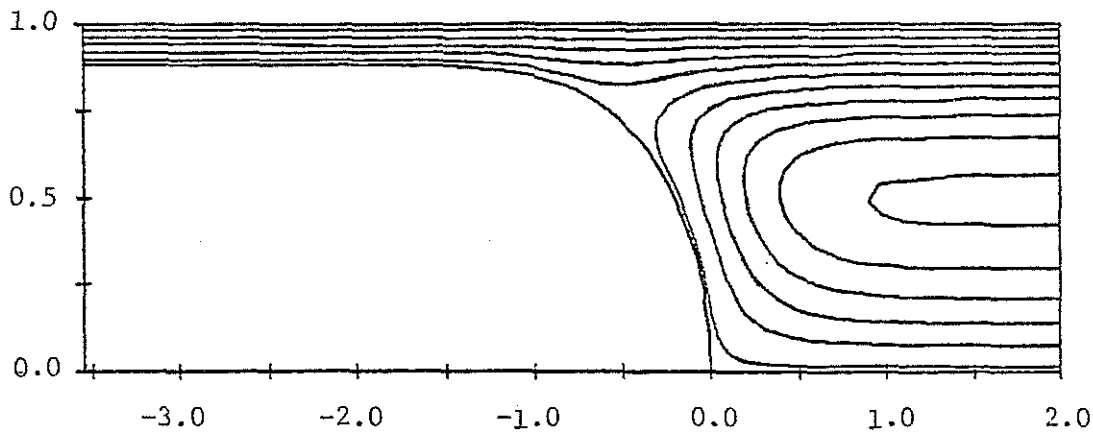

Figure 6b

Contour Plot of the Stream Function ψ

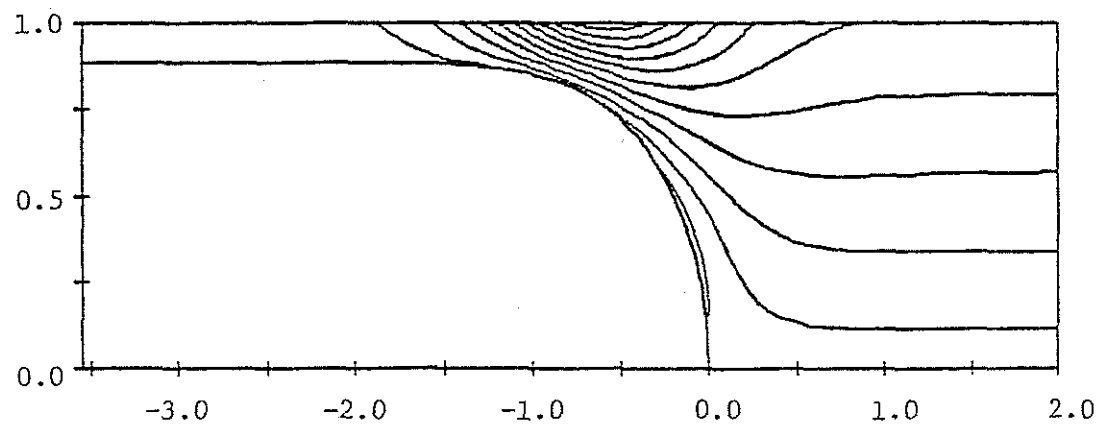

Figure 6c

Contour Plot of the Vorticity w

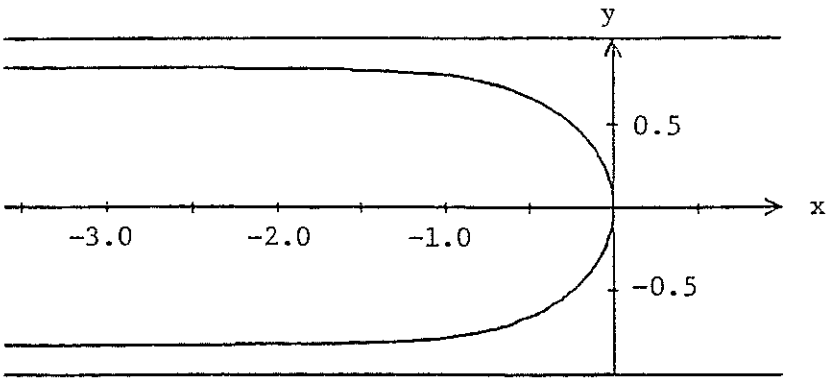

Figure 7a

Two-dimensional Finger Profile $\mu U/T = 0.10$

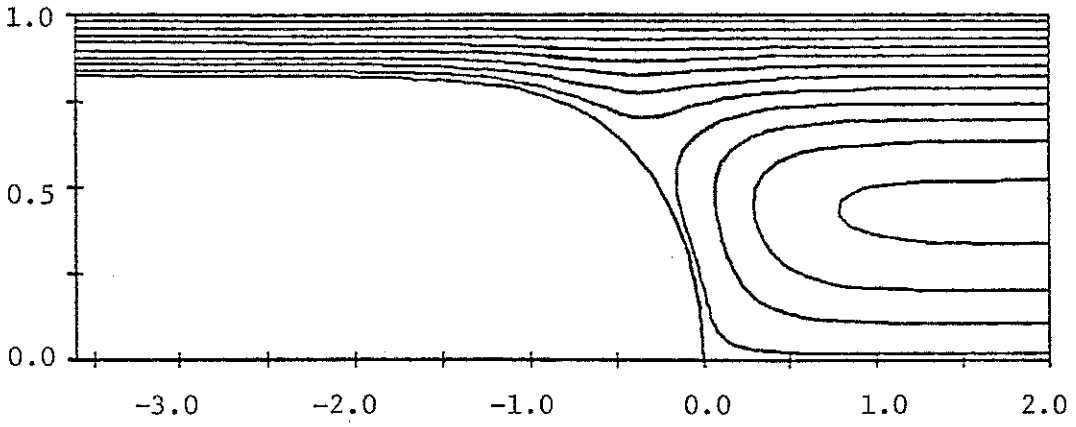

Figure 7b

Contour Plot of the Stream Function ψ

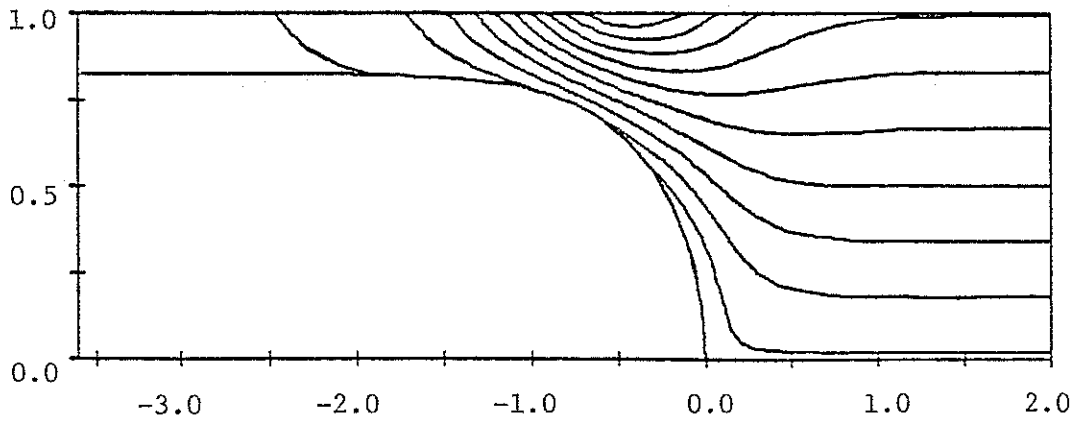

Figure 7c

Contour Plot of the Vorticity w

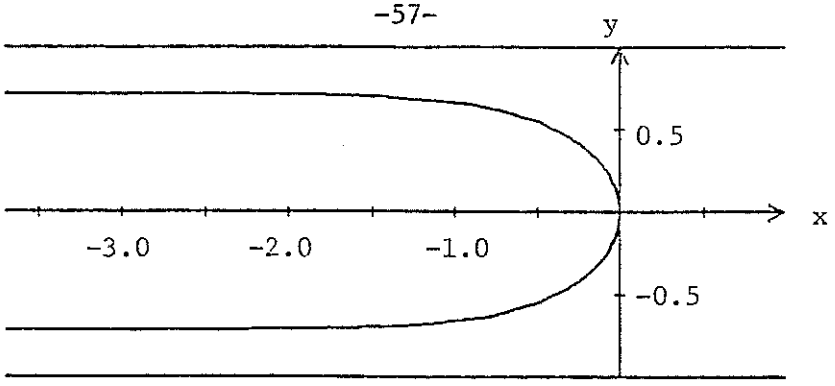

Figure 8a

Two-dimensional Finger Profile $\mu U/T = 0.40$

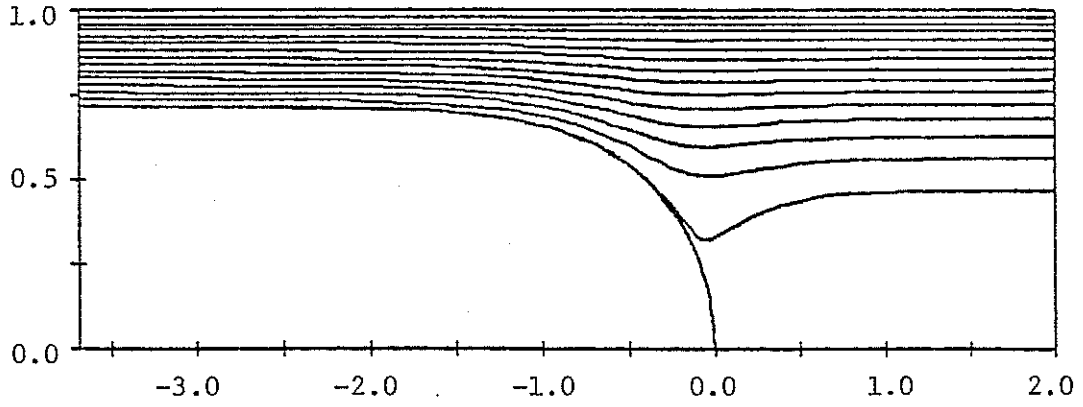

Figure 8b

Contour Plot of the Stream Function ψ

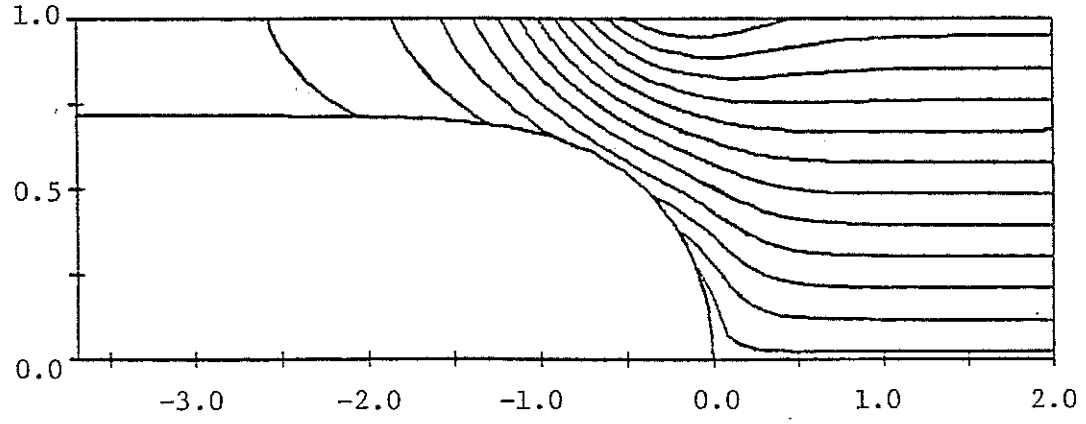

Figure 8c

Contour Plot of the Vorticity w

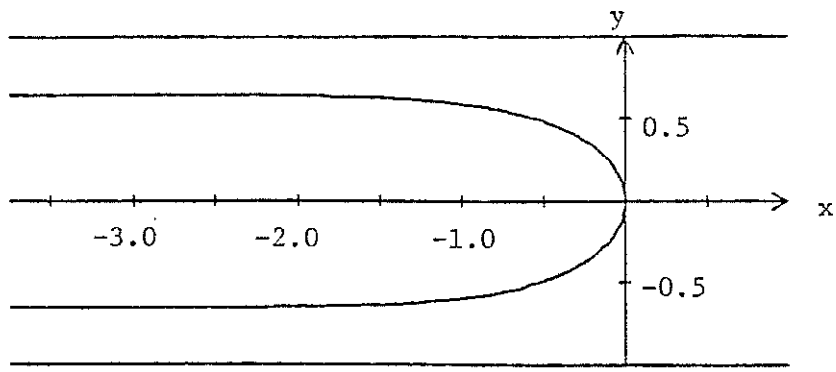

Figure 9a

Two-dimensional Finger Profile $\mu U/T = 1.00$

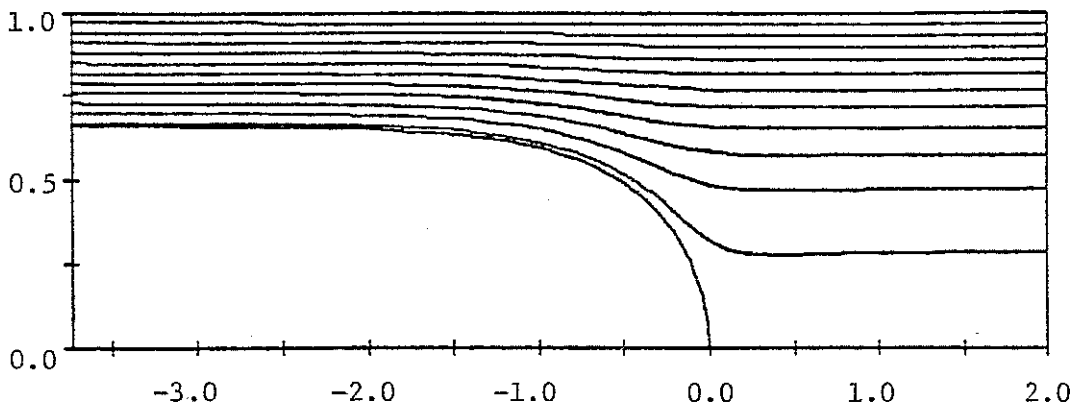

Figure 9b

Contour Plot of the Stream Function ψ

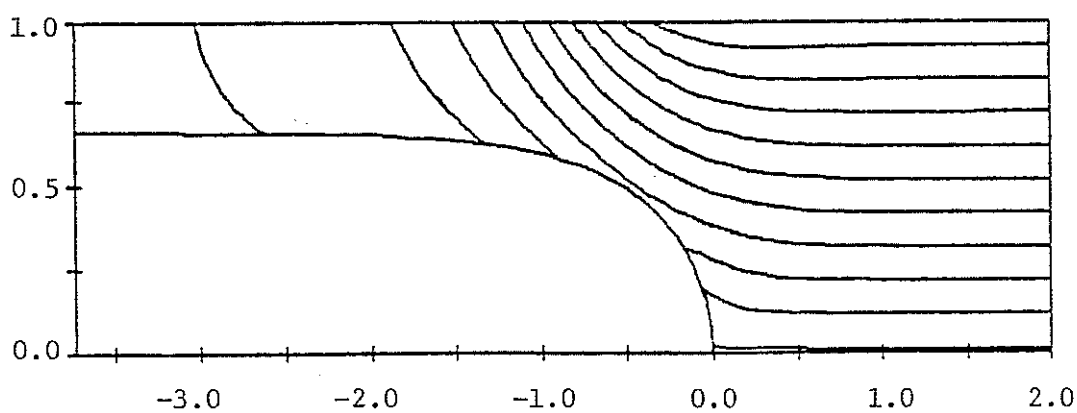

Figure 9c

Contour Plot of the Vorticity w

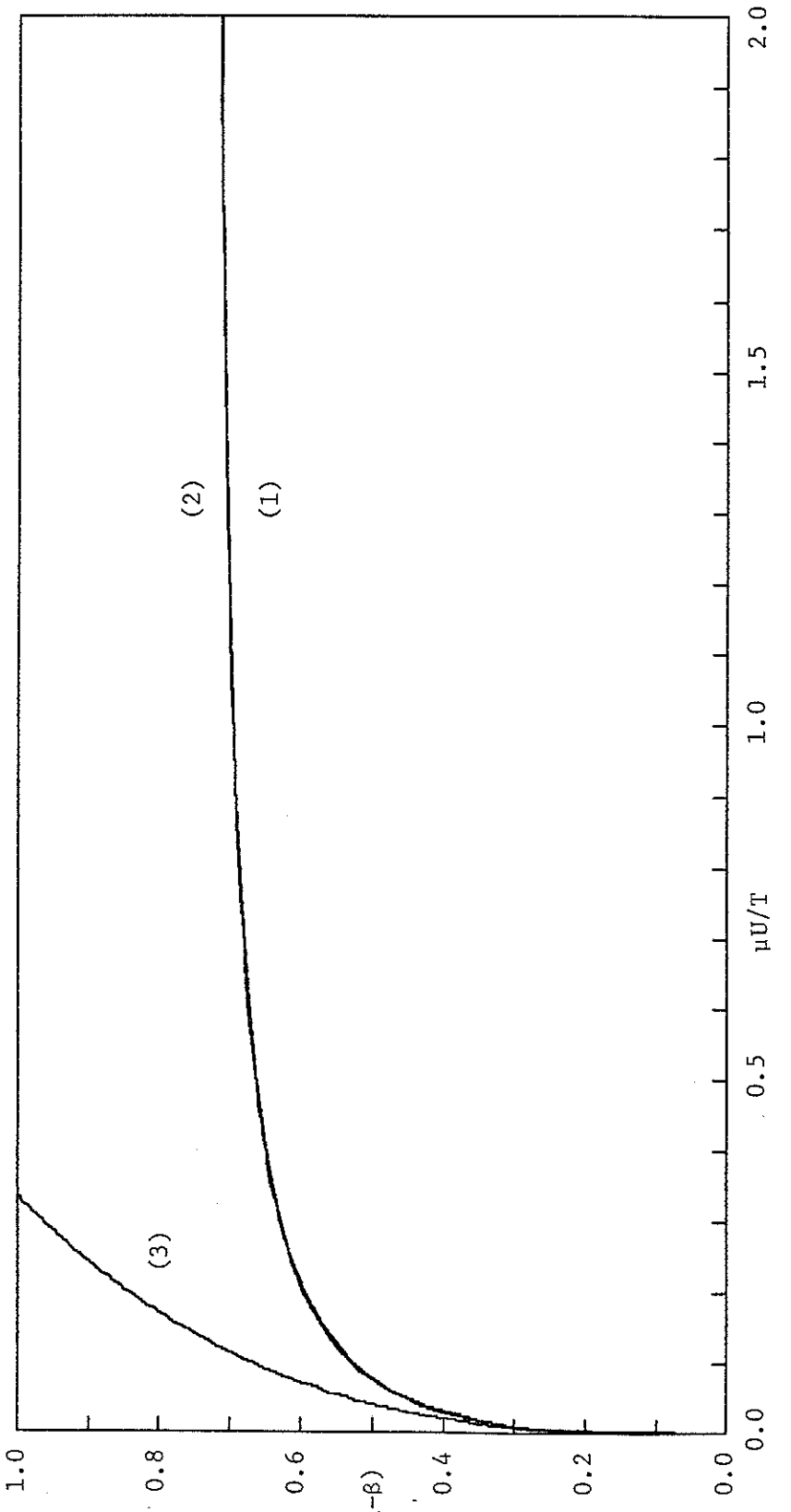

Figure 10

(1) Numerical Solution (2) Plot of Equation (26) (3) Perturbation Solution

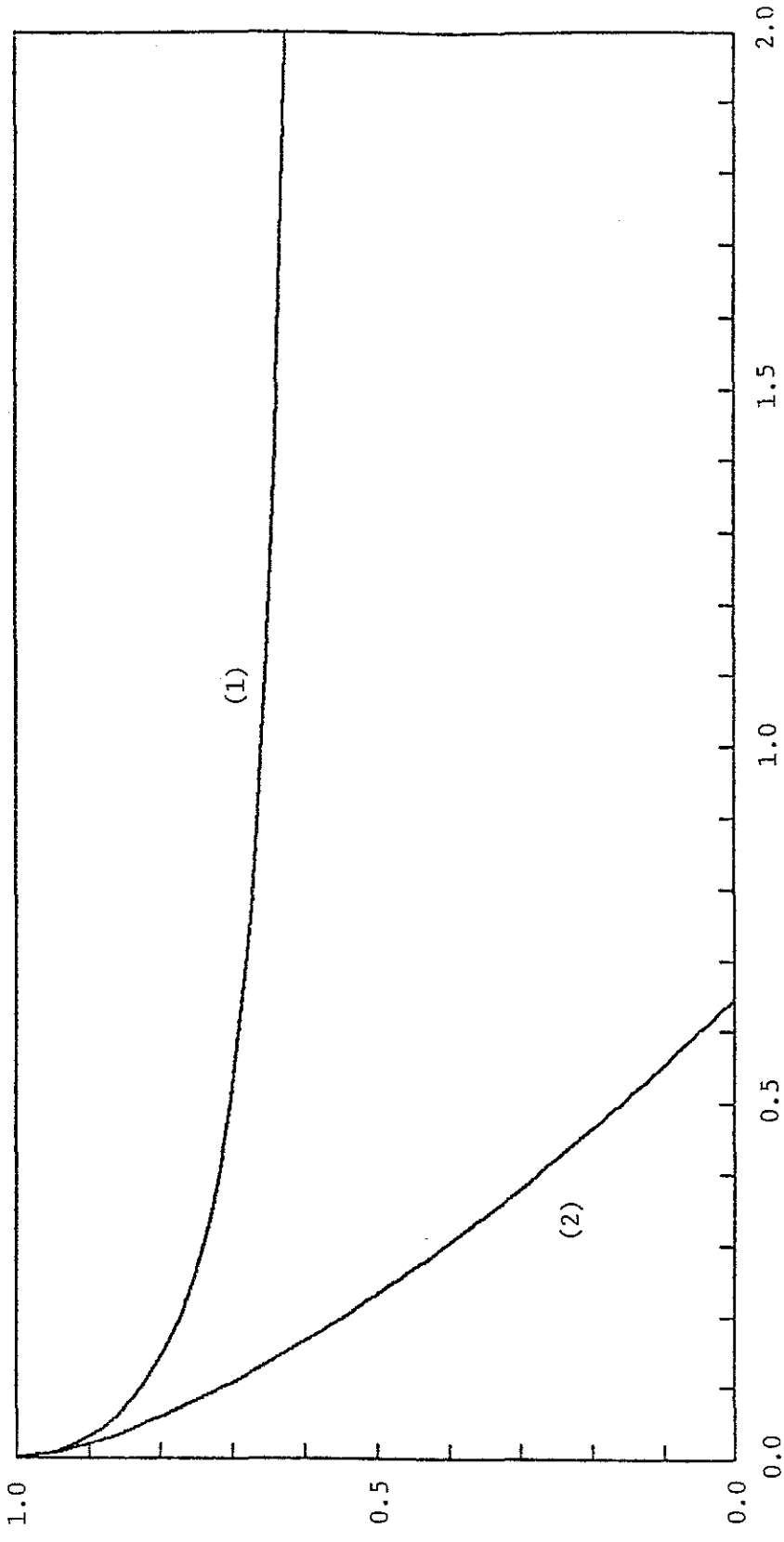

Figure 11

Two-dimensional Solution (1) Numerical Solution (2) Perturbation Solution

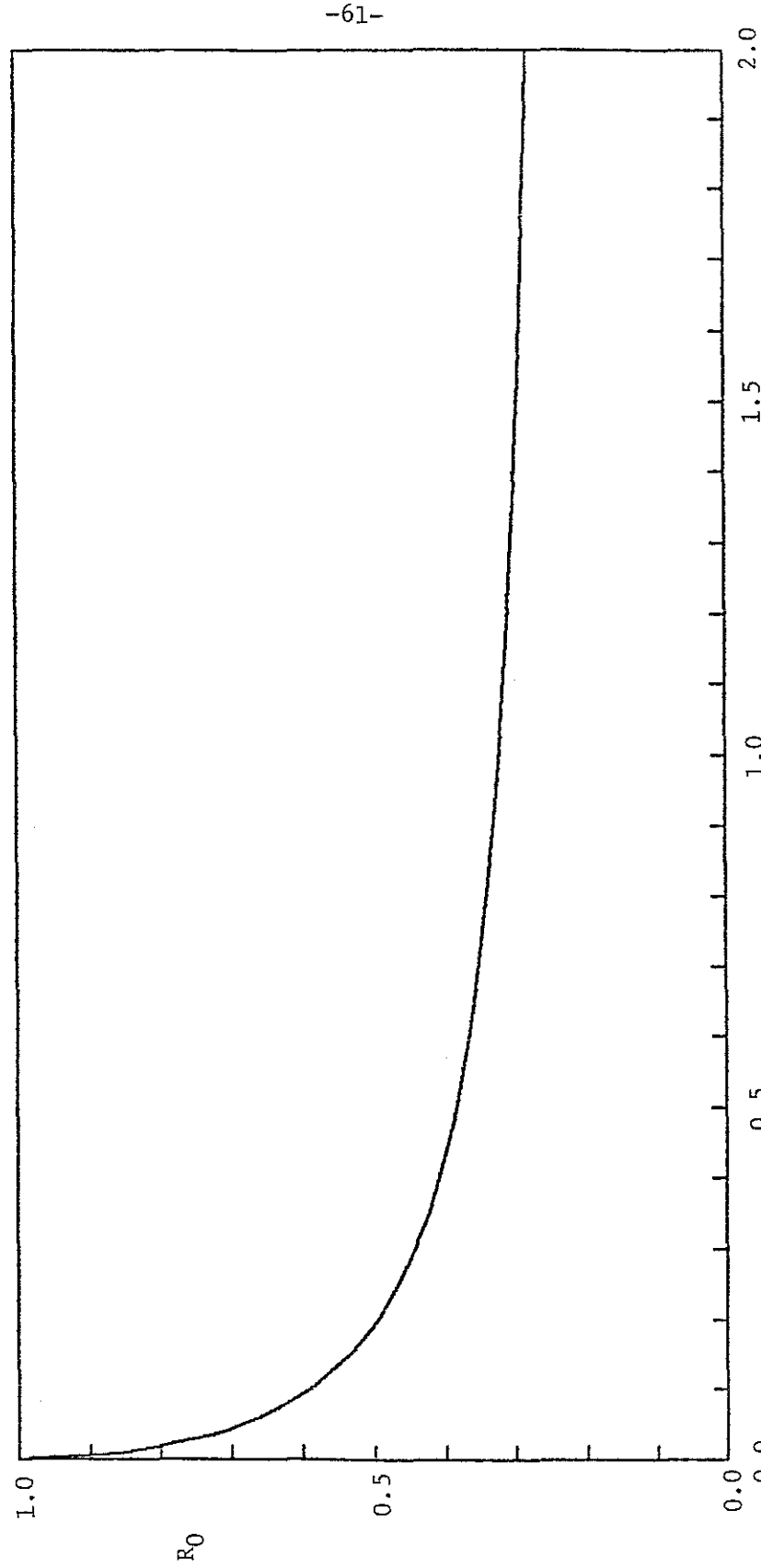

Figure 12
Two-dimensional Solution

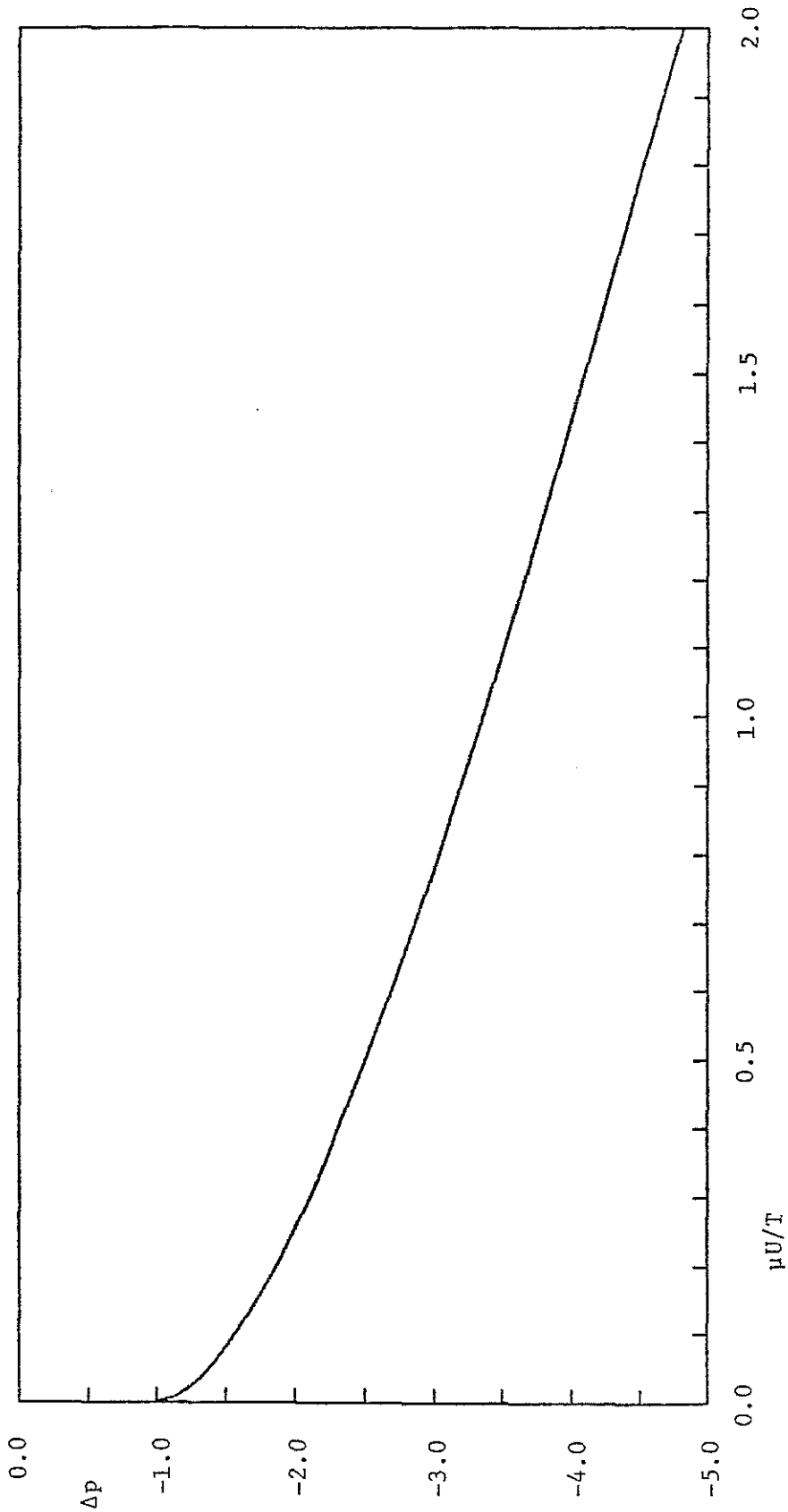

Figure 13
Two-dimensional Solution

V. Numerical Solution of the Axisymmetric Problem

5.1 Formulation of the Problem

In this chapter, we consider the penetration of a finger into a tube initially filled with a viscous fluid. As in the two-dimensional case, the steady state problem is examined and the finger moves parallel to the x-axis with constant velocity U. The diameter of the tube is $2b$ and the diameter of the finger is $2\beta b$. The parameter β is equal to (diameter of finger)/(diameter of tube).

Dimensionless variables are introduced in a form similar to that of the two-dimensional case. The assumption that the inertia terms can be neglected in comparison with the viscous terms is also made. Under this assumption, the conservation and momentum equations for incompressible axisymmetric flow that correspond to equations (2a,b,c) are given by

$$u_x + \frac{1}{y}(y\,v)_y = 0$$

$$p_x = Ca\left[u_{xx} + \frac{1}{y}(y\,u_y)_y\right] \qquad (57a,b,c)$$

$$p_y = Ca\left[v_{xx} + \frac{1}{y}(y\,v_y)_y - \frac{v}{y^2}\right]$$

The variable y is used for the radial coordinate to avoid confusion with the r coordinate used in the curvilinear grid. The geometry of the problem is identical to Figure 2.

The stream function ψ is defined by

$$u = \frac{1}{y}\psi_y \qquad v = -\frac{1}{y}\psi_x$$

and the vorticity w defined by

$$w = u_y - v_x$$

These expressions are substituted into equations (57a,b,c). The pressure is eliminated from the equations to give

$$\psi_{xx} + \psi_{yy} - \frac{1}{y}\psi_y = y\,w$$
$$w_{xx} + w_{yy} + \frac{1}{y}w_y - \frac{1}{y^2}w = 0 \qquad (58a,b)$$

The interface is described by $(x(s,0), y(s,0))$ where s is the arclength along the interface curve. In the axisymmetric case, the boundary conditions on the interface are given by

$$\psi = 0$$
$$y\,w + 2\,x_{ss}\,\psi_x + 2\,y_{ss}\,\psi_y = 0 \qquad (59a,b,c)$$
$$p - 2\,Ca\left[y_s^2 u_x - x_s\,y_s\,(v_x + u_y) + x_s^2 v_y\right] = p_0 - \left(\frac{1}{R_1} + \frac{1}{R_2}\right)$$

where

$$u_x = \frac{1}{y}\psi_{xy} \qquad u_y = \frac{1}{y}\psi_{yy} - \frac{1}{y^2}\psi_y$$
$$v_x = -\frac{1}{y}\psi_{xx} \qquad v_y = -\frac{1}{y}\psi_{xy} + \frac{1}{y^2}\psi_x \qquad (60a,b,c,d)$$

The principal curvatures for the axisymmetric problem are

$$\frac{1}{R_1} = x_s\,y_{ss} - y_s\,x_{ss} \qquad \frac{1}{R_2} = -\frac{x_s}{y}$$

The pressure p_0 is the pressure inside the finger and is set equal to zero. The

boundary conditions on the wall of the tube are

$$\psi(x,1) = -\tfrac{1}{2}(1-\beta^2) \qquad \psi_y(x,1) = -1$$

and the symmetry conditions on the centerline are

$$\psi(x,0) = 0 \qquad w(x,0) = 0$$

The asymptotic behavior of ψ and w as $x \to -\infty$ is

$$\psi \to -\tfrac{1}{2}(y^2-\beta^2) \qquad w \to 0$$

and the behavior as $x \to \infty$ is

$$\psi \to \tfrac{1}{2}\beta^2(2y^2-y^4)-\tfrac{1}{2}y^2 \qquad w \to -4\beta^2 y$$

As in the two-dimensional case, the normal-stress boundary condition is dropped, and the numerical solution is computed on a fixed domain. The pressure is calculated from the vorticity solution by integrating along the interface

$$\begin{aligned} p_s &= x_s p_x + y_s p_y \\ &= Ca\, x_s \left[w_y + \frac{w}{y}\right] + Ca\, y_s \left[-w_x\right] \\ &= Ca\, x_s \left[s_y w_s + r_y w_r\right] - Ca\, y_s \left[s_x w_s + r_x w_r\right] + \frac{Ca\, x_s\, w}{y} \\ &= Ca \left[x_s r_y - y_s r_x\right] w_r + Ca \left[x_s s_y - y_s s_x\right] w_s + \frac{Ca\, x_s\, w}{y} \end{aligned}$$

The values of the derivatives of ψ are computed at each grid point on the interface as in section 4.3. The stresses are now calculated using equations (60a,b,c,d). At the tip of the finger, it is necessary to examine the stresses in

the limit as $y \to 0$. The interface is expanded using Tchebycheff polynomials and equation (55).

5.2 Numerical Results and Comparison with Experiments

The curvilinear and rectilinear grids used for the axisymmetric problem are the same as those used in the two-dimensional case for a given value of $\mu U/T$. Table 4 gives the values of β, R_0, and Δp at each value of $\mu U/T$ for which the numerical solution is determined. R_0 is equal to the radius of curvature at the tip of the finger which is equal to both R_1 and R_2. R_0 has been normalized by b. Δp is the pressure drop across the tip of the finger which has been normalized by T/b. Finger profiles and contour plots of the stream function and the vorticity are shown in Figures 14, 15, 16, and 17 for $\mu U/T$ equal to 0.04, 0.10, 0.40, and 1.00. As $x \to \infty$, the velocity in the x-direction is

$$u \to 2\beta^2(1-y^2)-1$$

For β greater than $\frac{1}{\sqrt{2}}$, the fluid near the x-axis moves faster than the finger. Taylor [15] discusses the two simplest types of flows that might occur: a stagnation point at the origin with a stagnation ring on the interface of the finger or two stagnation points on the x-axis, one of which is at the origin. By examining the contour plots for the stream function, it is clear that a stagnation ring is present for β greater than $\frac{1}{\sqrt{2}}$. Figures 18, 19, and 20 are plots of β, R_0, and Δp versus $\mu U/T$. There are no major differences between the two-dimensional and axisymmetric results.

When the axisymmetric finger moves through the tube, a fraction m of the viscous fluid is left behind on the walls of the tube. The fraction m was measured experimentally by Taylor as a function of $\mu U/T$. Figure 21 compares the numerical results with the experimental results where m is equal to $1-\beta^2$. The numerical results are in excellent agreement with the experimental results.

$\mu U/T$	β	R_0	Δp
0.01	0.947	0.855	-2.29
0.02	0.922	0.792	-2.43
0.04	0.889	0.712	-2.65
0.06	0.866	0.659	-2.82
0.08	0.848	0.620	-2.97
0.10	0.833	0.590	-3.10
0.15	0.806	0.536	-3.40
0.20	0.786	0.500	-3.65
0.25	0.772	0.473	-3.89
0.30	0.760	0.452	-4.10
0.35	0.749	0.437	-4.30
0.40	0.741	0.424	-4.49
0.50	0.728	0.403	-4.85
0.60	0.718	0.388	-5.20
0.70	0.710	0.376	-5.53
0.80	0.703	0.366	-5.85
0.90	0.698	0.358	-6.16
1.00	0.694	0.351	-6.47
1.20	0.686	0.341	-7.06
1.40	0.681	0.331	-7.65
1.60	0.676	0.325	-8.23
1.80	0.673	0.320	-8.79
2.00	0.670	0.315	-9.36
3.00	0.660	0.301	-12.13

Table 4

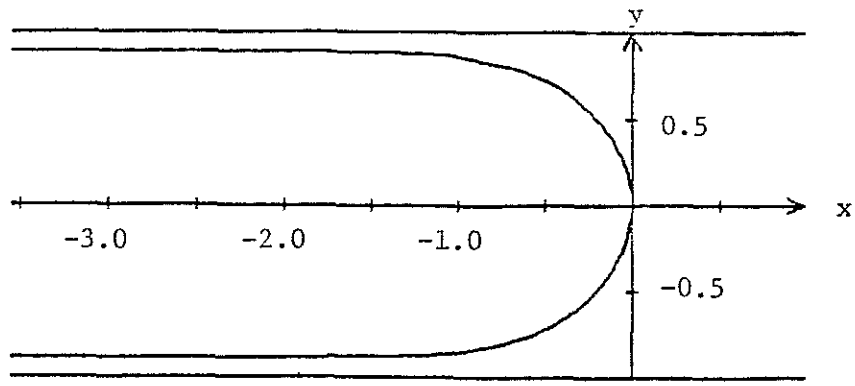

Figure 14a

Axisymmetric Finger Profile $\mu U/T = 0.04$

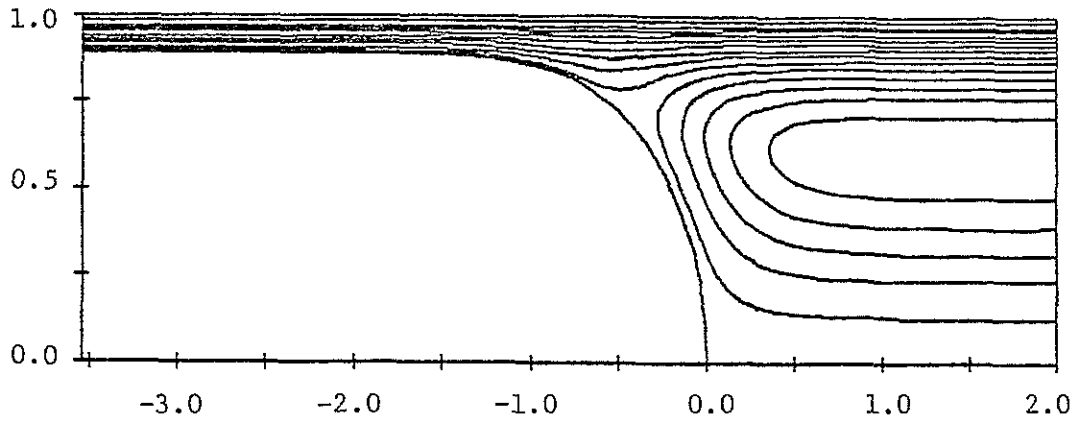

Figure 14b

Contour Plot of the Stream Function ψ

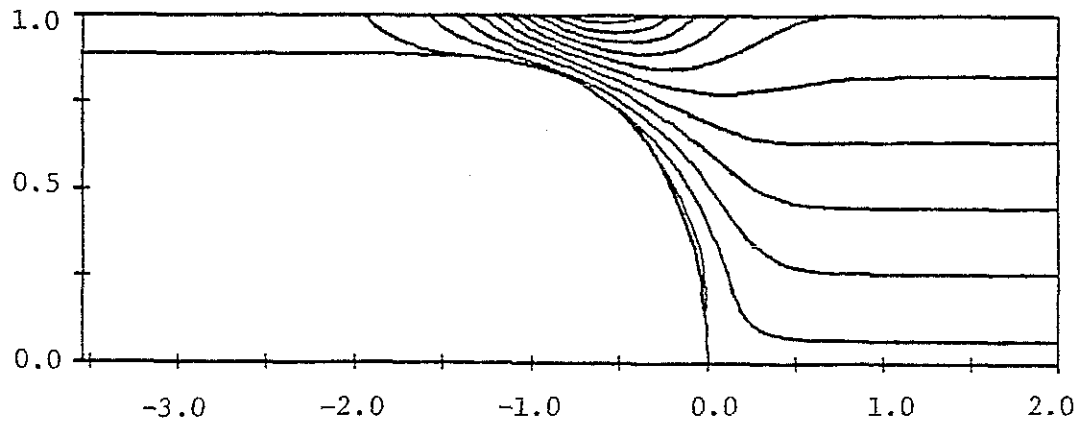

Figure 14c

Contour Plot of the Vorticity w

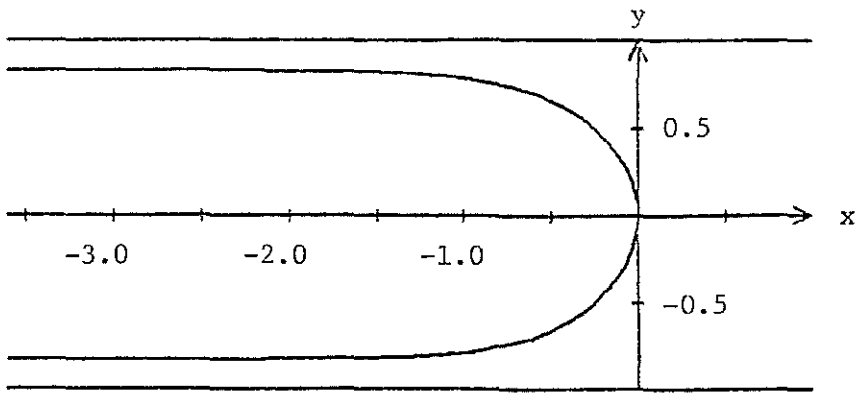

Figure 15a

Axisymmetric Finger Profile $\mu U/T = 0.10$

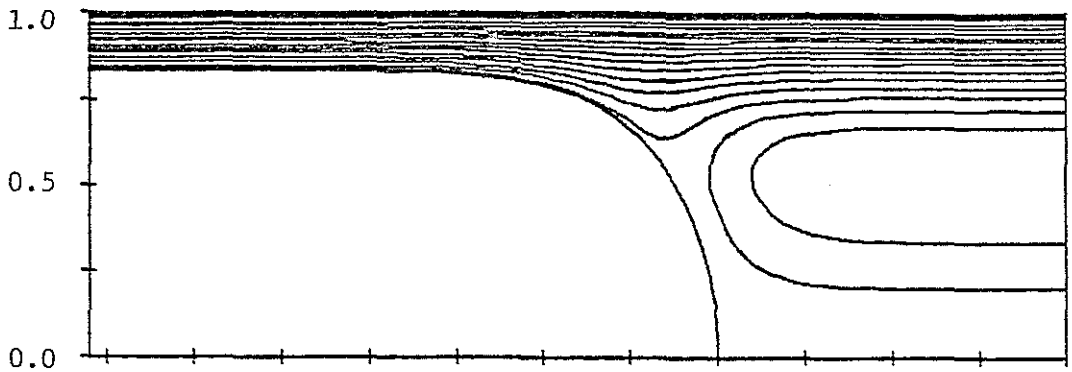

Figure 15b

Contour Plot of the Stream Funcion ψ

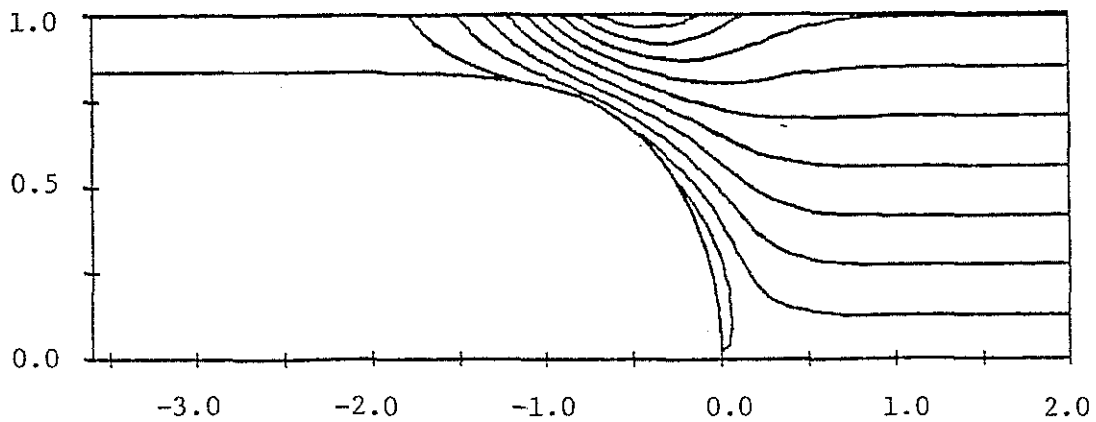

Figure 15c

Contour Plot of the Vorticity w

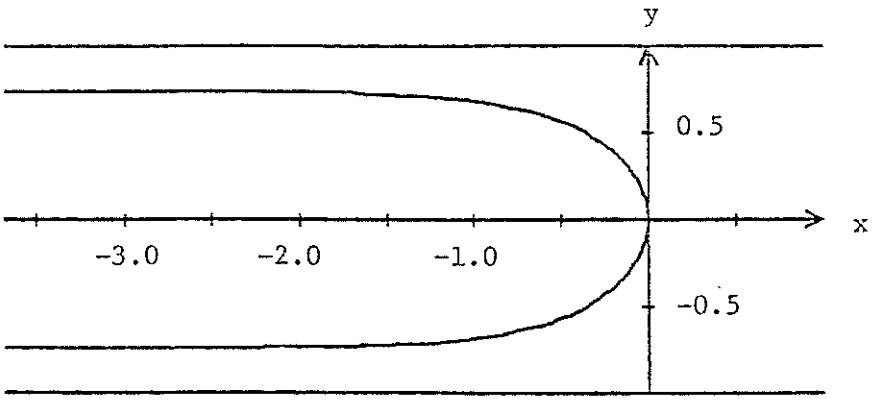

Figure 16a

Axisymmetric Finger Profile $\mu U/T = 0.40$

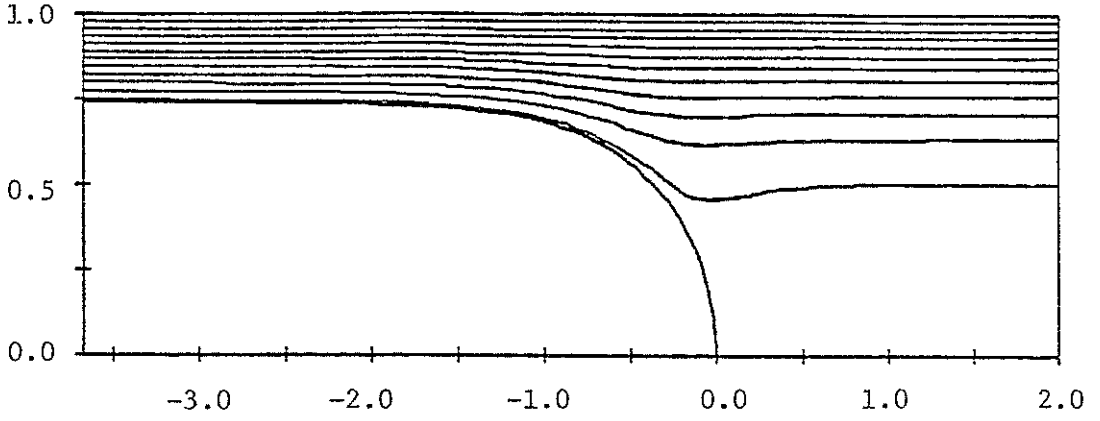

Figure 16b

Contour Plot of the Stream Function ψ

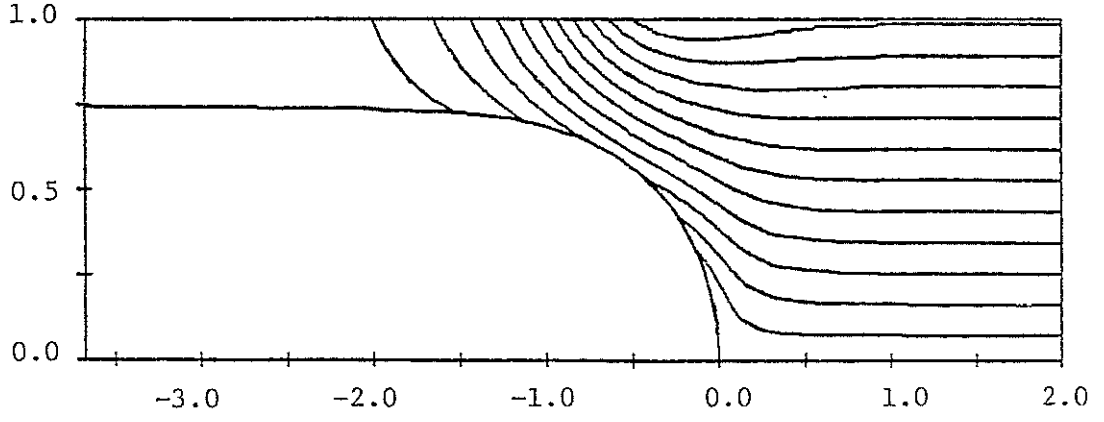

Figure 16c

Contour Plot of the Vorticity w

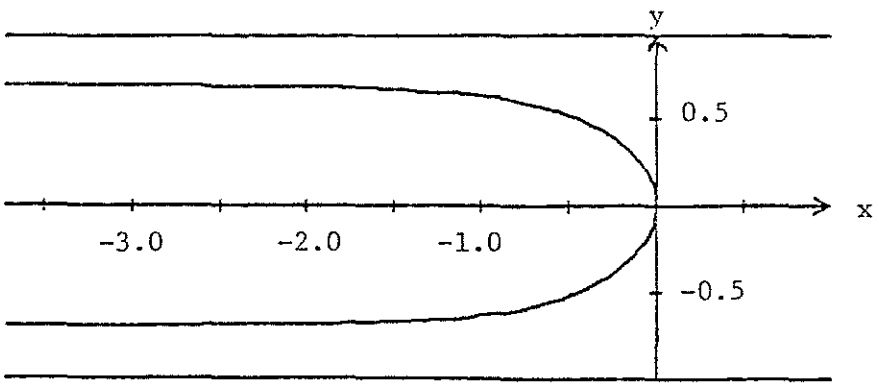

Figure 17a

Axisymmetric Finger Profile $\mu U/T = 1.00$

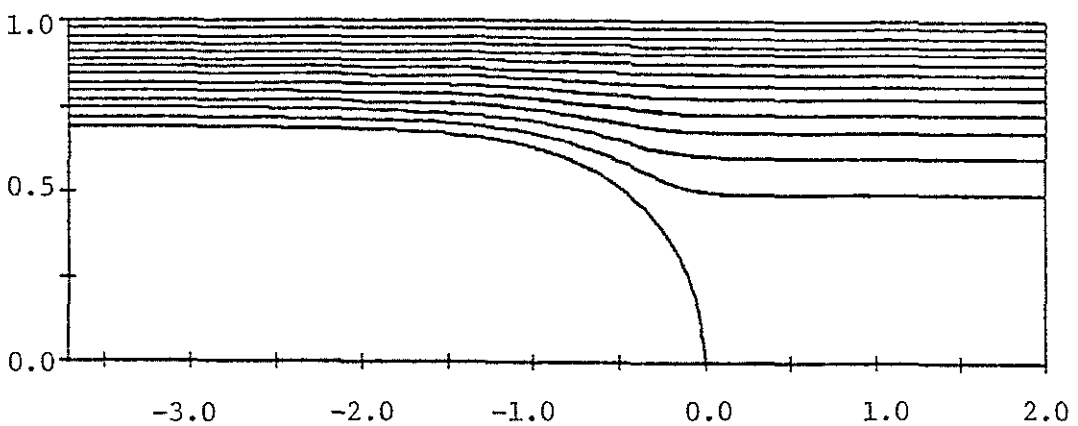

Figure 17b

Contour Plot of the Stream Function ψ

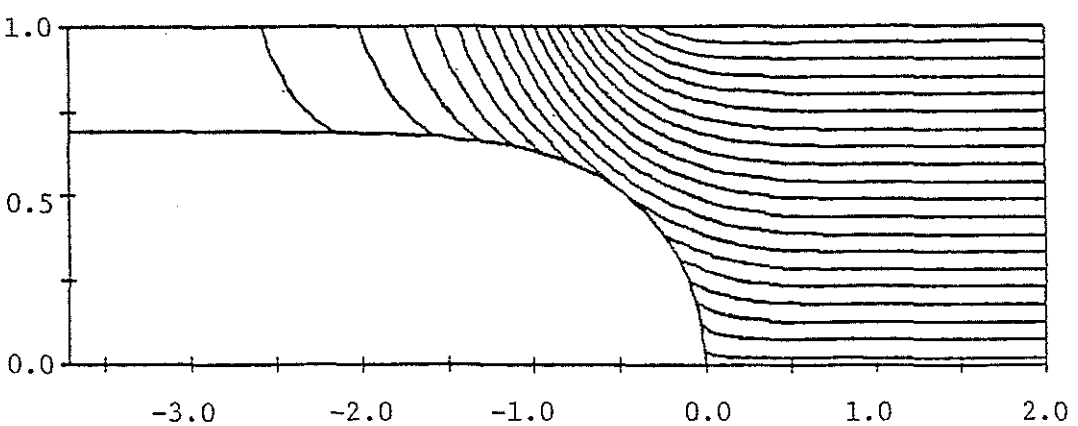

Figure 17c

Contour Plot of the Vorticity w

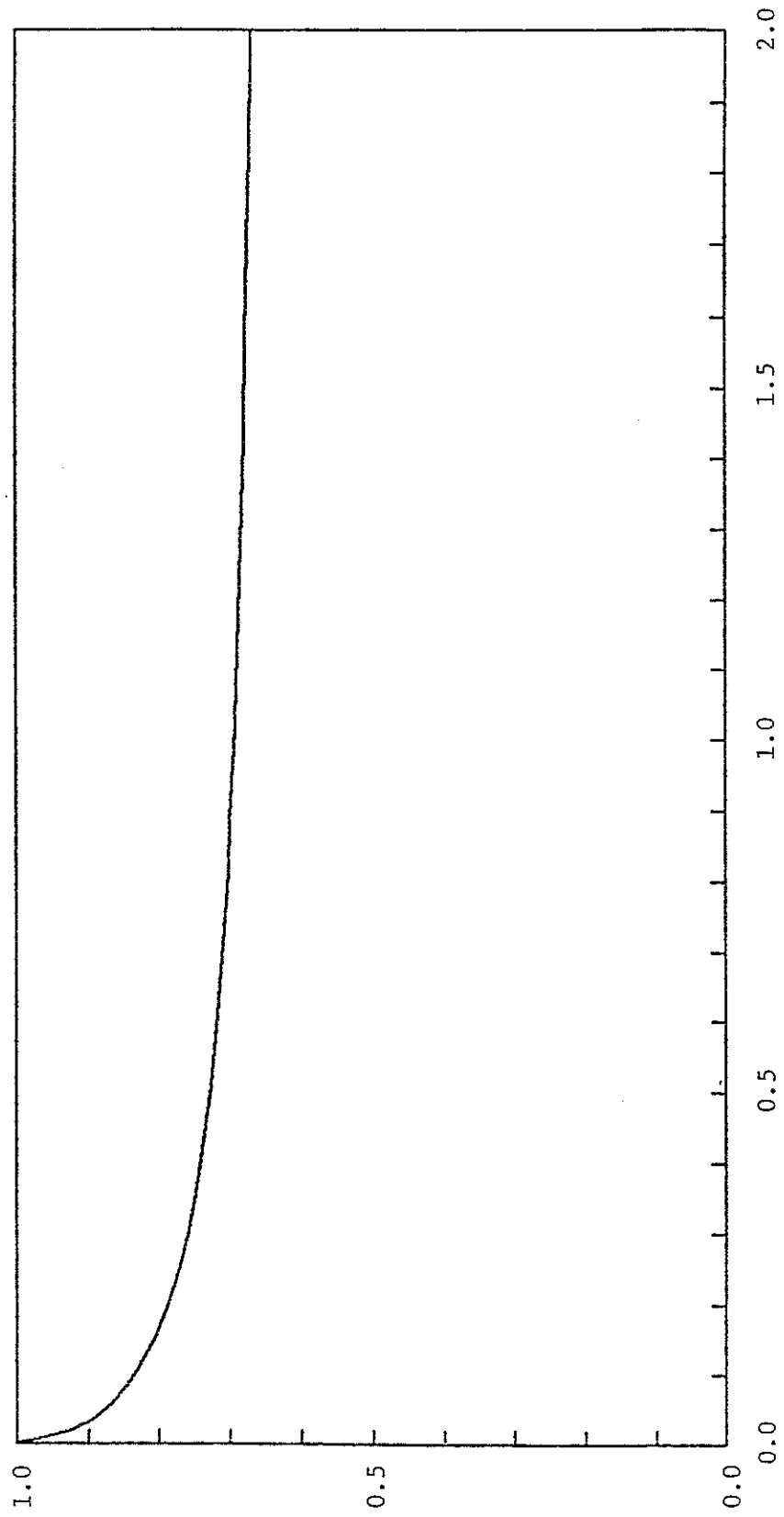

Figure 18
Axisymmetric Solution

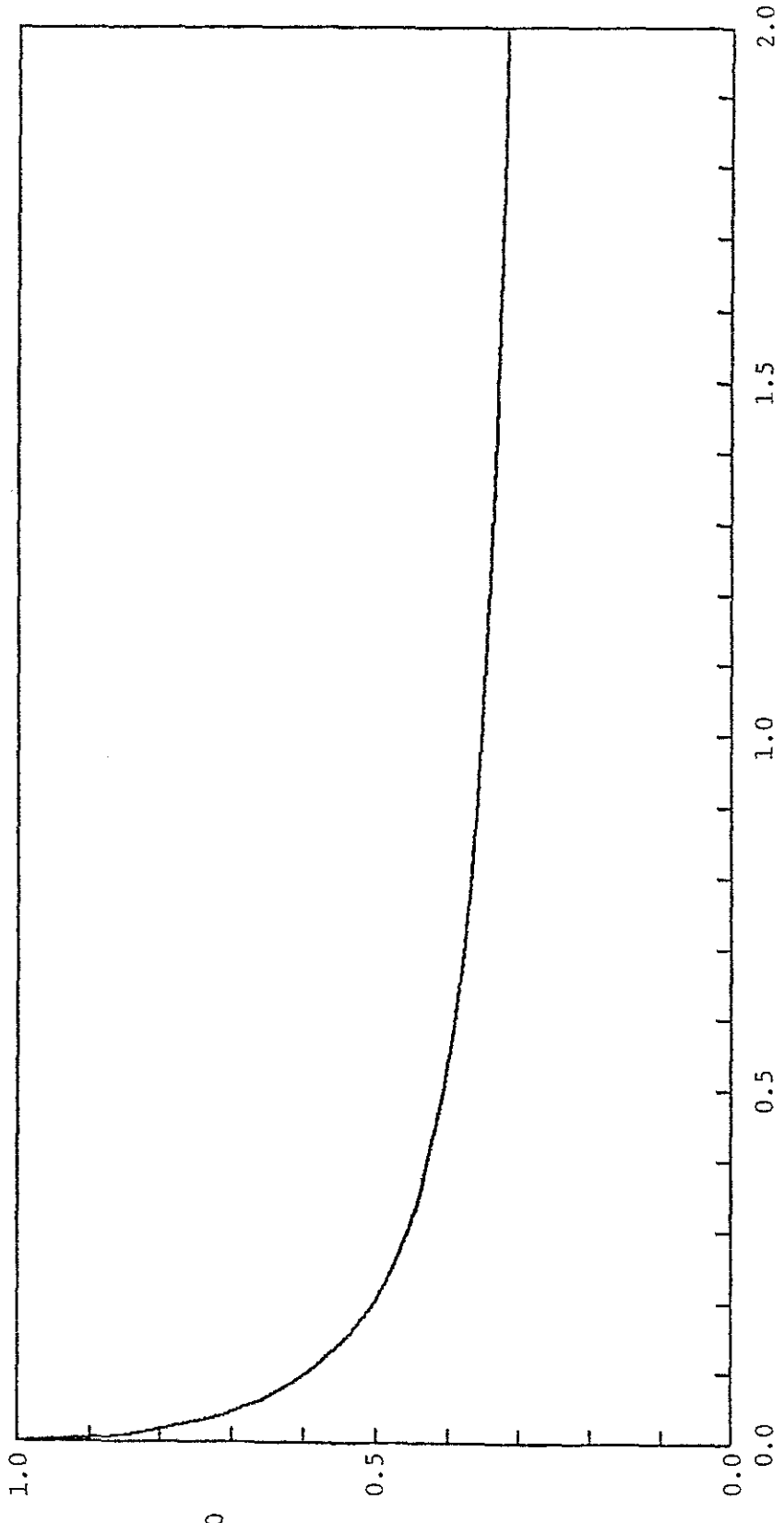

Figure 19
Axisymmetric Solution

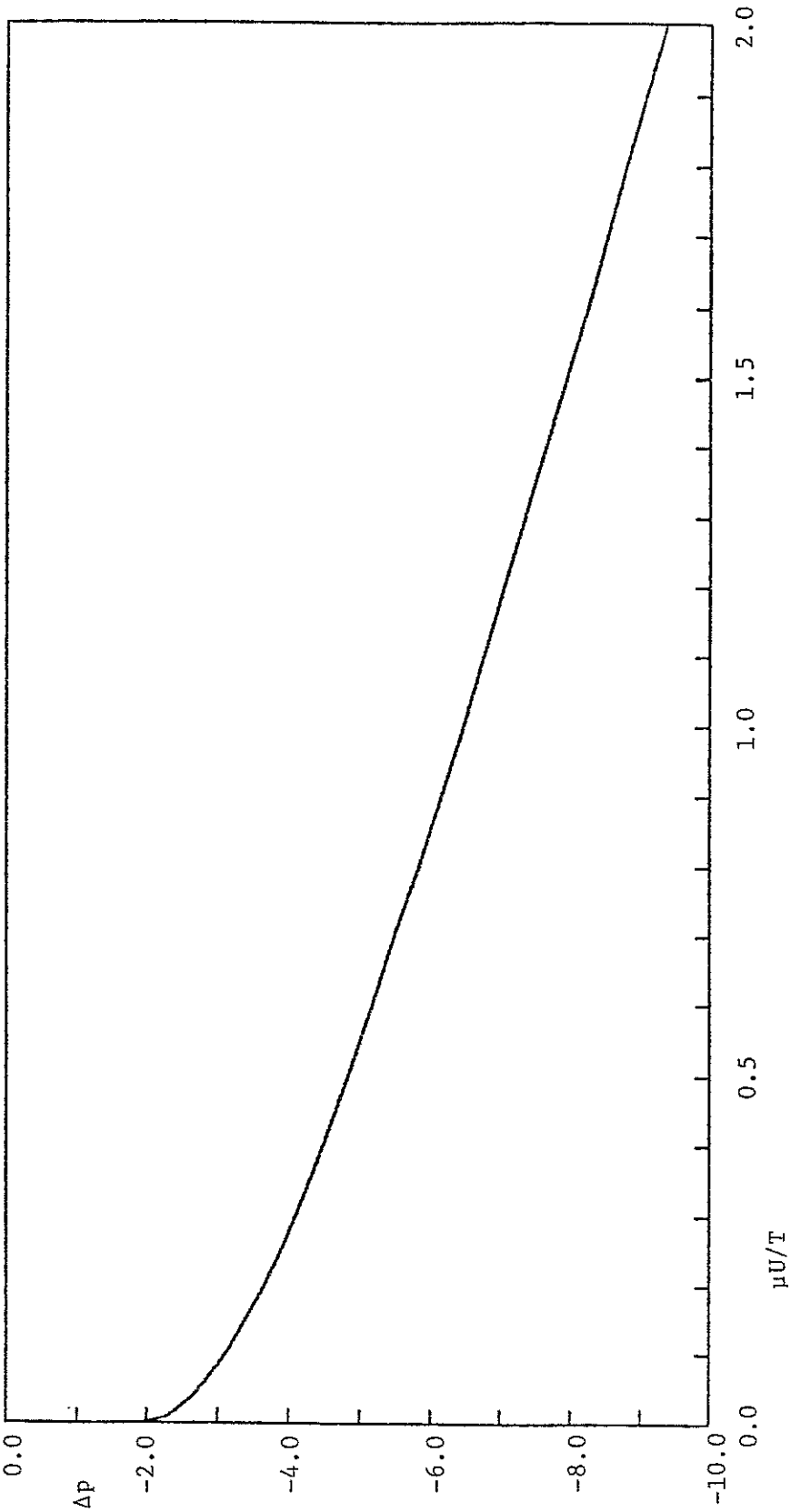

Figure 20
Axisymmetric Solution

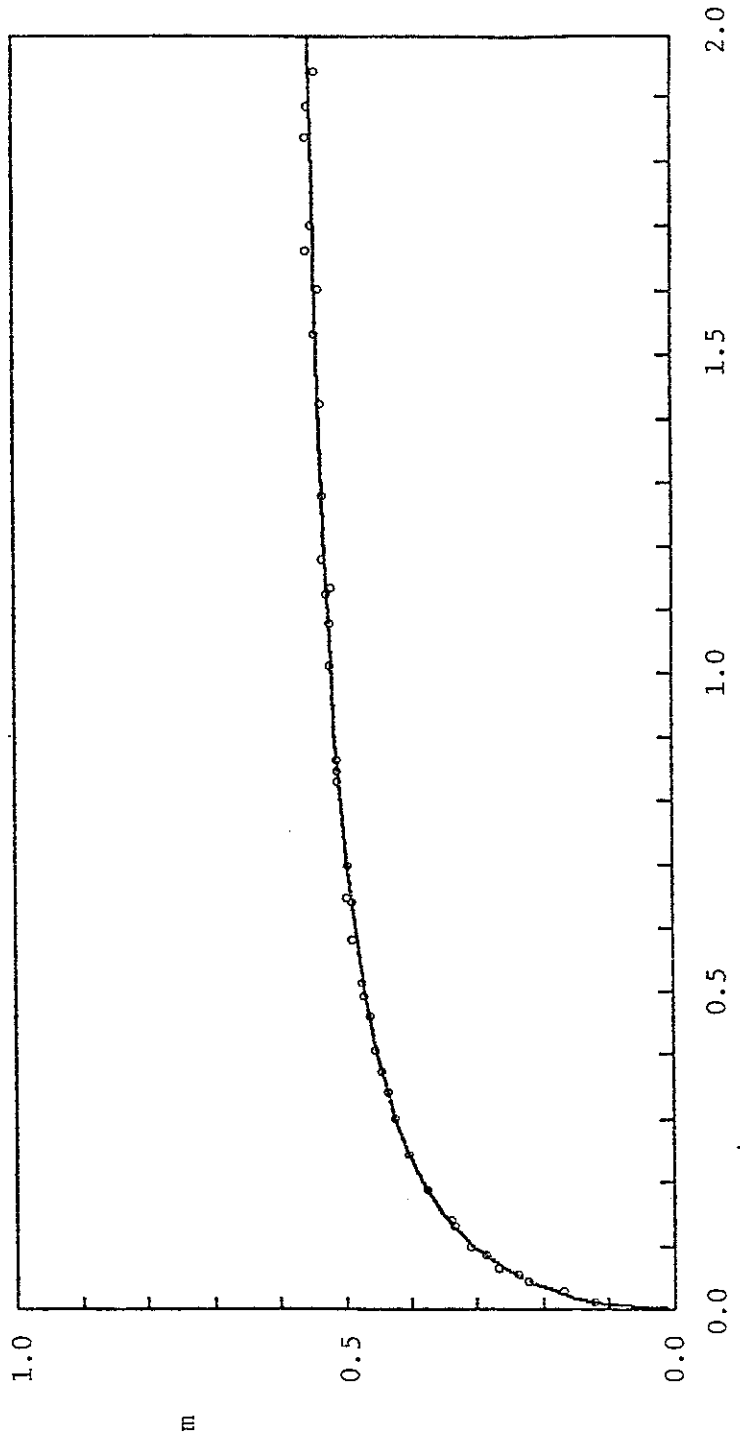
1.0
0.5
0.0
m
0.0
0.5
1.0
1.5
2.0
μU/T
— Axisymmetric Solution
∘ Experimental Results (Taylor)

Figure 21

VI. Discussion

In solving the fingering problem, we have used a composite mesh to cover the domain. The resulting numerical solution is not only accurate in the interior of the region but also on the boundaries of the domain. The amount of computing time necessary to construct the grids is a very small percentage of the time necessary to compute the solution to the fingering problem.

The employment of a composite mesh creates enough flexibility that it can be used to treat problems with many different types of geometries. It can also be used in determining solutions that exhibit singular behavior. The composite mesh can be composed of as many grids as necessary to solve a given problem. The grids are easily constructed to include stretching which places more grid points where they are needed most.

In this thesis, the solution is calculated by solving a large sparse system of equations that includes the solution on both the rectilinear and curvilinear grid. If we had used a single grid to solve the problem, then the sparse matrix would be a band matrix. When two grids are used, interpolation equations are needed to connect the solution on the different grids. The interpolation equations change the structure of the sparse matrix such that it is no longer a band matrix. This increases the storage and computation time needed to solve the system of equations. It would be useful to solve a smaller system of equations on each grid separately and then iterate back and forth between the two grids until the correct solution to the entire problem is determined. The smaller system of equations on each grid is banded and thus could be solved more quickly. This could be done for Laplace's equation using the interpolation formulas used

for the fingering problem. It should be noted that the convergence rate would depend on the size of the overlap region of the two grids.

The numerical methods employed in this thesis work very well in the treatment of a free surface problem. Many other free surface problems could be examined by extending the methods to include the effects of the inertia terms. The methods could also be extended to handle time-dependent free surface problems. In these problems, the curvilinear grid would move with the interface at each time step of the calculation.

There are various fingering problems that can be examined using these methods. The effects of gravity on the shape of the finger for the two-dimensional and axisymmetric geometries can be calculated. Now that we have solved the two-dimensional problem between the plates, we can apply the results to possibly improve the interface boundary condition used to examine the finger in the plane parallel to the plates of the Hele-Shaw cell. It is hoped that an improved interface condition will bring the plot of λ versus $\mu U/T$ into agreement with experiments.

Appendix

To fully understand the problems associated with using the computational boundary conditions given at the beginning of section 4.2, we examine equations (48a,b)

$$\psi_{xx} + \psi_{yy} = w$$
$$w_{xx} + w_{yy} = 0$$

on a rectangular domain given by $0 \leq x \leq x_0$ and $0 \leq y \leq 1$. One solution of the equations is

$$\psi(x,y) = y \cosh y \sin x$$
$$w(x,y) = 2 \sinh y \sin x$$

To solve this problem numerically, the appropriate values of ψ and w are specified on all boundaries except $y = 1$ where ψ and ψ_y are given. The following five point difference equation is used for the two partial differential equations:

$$\psi_{xx} + \psi_{yy} = \frac{\psi_{i+1,j} - 2\psi_{i,j} + \psi_{i-1,j}}{h_x^2} + \frac{\psi_{i,j+1} - 2\psi_{i,j} + \psi_{i,j-1}}{h_y^2}$$

The grid is constructed with the boundary $y = 1$ centered between the top two grid lines. This allows us to give the following values of ψ on the top two grid lines:

$$\psi_{i,N_y} = \psi\left(x_i, 1 + \frac{h_y}{2}\right) = \psi(x_i,1) + \frac{h_y}{2}\psi_y(x_i,1)$$

$$\psi_{i,N_y-1} = \psi\left(x_i, 1 - \frac{h_y}{2}\right) = \psi(x_i,1) - \frac{h_y}{2}\psi_y(x_i,1)$$

where h_y is the mesh size in the y direction. The leading order error in applying these two boundary conditions is equal to $\frac{1}{8}h_y^2\psi_{yy}(x_i,1)$.

To explicitly demonstrate that the vorticity error is $O(1)$ near the corner where $x=x_0$ and $y=1$, we calculate the vorticity w at the grid point (x_{N_x-1},y_{N_y-1}) using the difference equation for ψ. The value of ψ at each of the five grid points needed to calculate $\overline{w}=w_{N_x-1,N_y-1}$ can be expanded in terms of $\overline{\psi}=\psi_{N_x-1,N_y-1}$

$$\psi_{N_x-1,N_y}=\overline{\psi}+h_y\overline{\psi}_y+\frac{3}{8}h_y^2\overline{\psi}_{yy}+O(h_y^3)$$

$$\psi_{N_x-2,N_y-1}=\overline{\psi}-h_x\overline{\psi}_x+\frac{1}{2}h_x^2\overline{\psi}_{xx}-\frac{1}{8}h_y^2\overline{\psi}_{yy}+O(h_x^3,h_xh_y^2,h_y^3)$$

$$\psi_{N_x-1,N_y-1}=\overline{\psi}-\frac{1}{8}h_y^2\overline{\psi}_{yy}+O(h_y^3)$$

$$\psi_{N_x,N_y-1}=\overline{\psi}+h_x\overline{\psi}_x+\frac{1}{2}h_x^2\overline{\psi}_{xx}+O(h_x^3)$$

$$\psi_{N_x-1,N_y-2}=\overline{\psi}-h_y\overline{\psi}_y+\frac{1}{2}h_y^2\overline{\psi}_{yy}+O(h_y^3)$$

The first four values of ψ given above are specified by the boundary conditions. As discussed above, the first three values contain a leading order error equal to $\frac{1}{8}h_y^2\psi_{yy}(x_i,1)$. The last value ψ_{N_x-1,N_y-2} is determined by calculating the numerical solution to the problem. Due to numerical error, the actual computed value will differ slightly from the exact value given above. If we substitute the above expressions into the difference equation for ψ, we get

$$\overline{w}=\overline{\psi}_{xx}+\overline{\psi}_{yy}+\frac{1}{8}\overline{\psi}_{yy}\left[1+\frac{h_y^2}{h_x^2}\right]+o(1)$$

where an $O(1)$ error for the vorticity $\overline{w}$ is present. If we make the assumption

that the computational error for ψ_{N_x-1,N_y-2} is close to $\frac{1}{8}h_y^2\psi_{yy}(x_{N_x-1},1)$, then the $\frac{1}{8}\bar{\psi}_{yy}$ term in the expression for $\bar{w}$ will not be present. Even this assumption does not eliminate the $O(1)$ error in the vorticity.

We now consider a grid point on the grid line $y=1-\frac{h_y}{2}$ in the center of the interval $0\le x\le x_0$. In this case, all the values of ψ needed to calculate the vorticity will have an error close to $\frac{1}{8}h_y^2\psi_{yy}(x_i,1)$. Since the error in ψ is a smooth function, the error in the vorticity is now $o(1)$. It is a discontinuity of $O(h^2)$ in the value of ψ that produces $O(1)$ errors in the vorticity.

We now determine the numerical solution which will demonstrate the problems discussed above. In the following tables $e_{\max}$ is the maximum error of the vorticity at any grid point. The location of the maximum error is (x_i,y_j) where the value of i and j are given in the tables. N_x and N_y are the number of grid points in the x and y directions. In table 5, ψ and w are given on all boundaries except on $y=1$ where ψ and ψ_y are given. For $x_0=1$, the error in the vorticity is $O(1)$ and changes only slightly as the mesh size is decreased. When $x_0=\pi$, the discontinuity in ψ, which is due to the computational boundary conditions, does not occur. The error in the vorticity is now $O(h^2)$. In this last case, the results are similar to those found when the boundary is a smooth curve.

In many problems which have equations similar to (48a,b), the values of ψ and ψ_n are given on the boundaries. The value of ψ will also have an $O(h^2)$ discontinuity at the corners for these boundary conditions. In Table 6, ψ and ψ_x are given on $x=x_0$, ψ and ψ_y are given on $y=1$, and ψ and w are given on the other boundaries. The boundary $x=x_0$ is centered between two grid lines. The computational boundary conditions used on $x=x_0$ have the same form as those applied on $y=1$. Again, the error in the vorticity is $O(1)$ near the upper right-

hand corner. If $x_0 = \pi$, then ψ_{yy}, ψ_{yyy}, and ψ_{xx} are all equal to zero in the corner where $x = \pi$ and $y = 1$; ψ_{xxx} is not equal to zero. This produces an $O(h_x^3)$ discontinuity in ψ for the numerical problem. The vorticity error near the corner should now be $O(h_x)$. This result is confirmed by examining Table 6.

Finally, we determine the solution by using the computational boundary conditions used for the fingering problem. The boundary $y = 1$ coincides with the top grid line of the mesh. The computational boundary conditions on $y = 1$ are

$$\psi = \psi(x_i, 1)$$

$$w = \psi_{xx}(x_i, 1) + \frac{-7\psi_{i,N_y} + 8\psi_{i,N_y-1} - \psi_{i,N_y-2}}{2h_y^2} + \frac{3\psi_y(x_i, 1)}{h_y}$$

The values of ψ and w are applied on the other boundaries. Table 7 gives the results of these calculations. The vorticity error is small.

x_0	N_x	N_y	h_x	h_y	e_{max}	i	j
1.0	9	9	.125	.133	0.578	8	8
1.0	17	17	.063	.065	0.551	16	16
1.0	33	33	.031	.032	0.540	32	32
π	26	9	.126	.133	3.17E-02	13	8
π	51	17	.063	.065	7.81E-03	26	16

Table 5

x_0	N_x	N_y	h_x	h_y	e_{max}	i	j
1.0	9	9	.133	.133	0.484	7	8
1.0	17	17	.065	.065	0.524	15	16
1.0	33	33	.032	.032	0.547	32	31
π	26	9	.128	.133	8.54E-02	25	7
π	51	17	.063	.065	4.37E-02	50	15

Table 6

x_0	N_x	N_y	h_x	h_y	e_{max}	i	j
1.0	9	9	.125	.125	4.23E-03	6	9
1.0	17	17	.063	.063	1.82E-03	14	17
1.0	33	33	.031	.031	8.41E-04	31	33

Table 7

References

[1] Batchelor, G. K. 1967 *An Introduction to Fluid Mechanics*, Cambridge University Press.

[2] Bretherton, F. P. 1960 The motion of long bubbles in tubes, *J. Fluids Mech.*, **10**, 166-188.

[3] Dahlquist, G. & Bjorck, A. 1974 *Numerical Methods*, Prentice-Hall.

[4] Happel, J. & Brenner, H. 1965 *Low Reynolds Number Hydrodynamics*, Prentice-Hall.

[5] Kreiss, B. 1983 Construction of a curvilinear grid, *SIAM J. Sci. Stat. Comput.*, **4**, 270-279.

[6] Lamb, H. 1932 *Hydrodynamics*, Sixth Edition, Dover.

[7] McLean, J. W. 1980 *Ph.D. Thesis*, California Institute of Technology, Dept. of Applied Math.

[8] Pitts, E. 1980 Penetration of fluid into a Hele-Shaw cell: the Saffman-Taylor experiment, *J. Fluid Mech.*, **97**, 53-64.

[9] Reyna, L. G. 1982 *Ph.D. Thesis*, California Institute of Technology, Dept. of Applied Math.

[10] Roache, P. J. 1976 *Computational Fluid Dynamics*, Hermosa Publishers.

[11] Romero, L. A. 1982 *Ph.D. Thesis*, California Institute of Technology, Dept. of Applied Math.

[12] Ruschak, K. J. & Scriven, L. E. 1977 Developing flow on a vertical wall, *J. Fluid Mech.*, **81**, 305-316.

[13] Saffman, P. G. & Taylor, G. I. 1958 The penetration of a fluid into a porous medium or Hele-Shaw cell containing a more viscous liquid, *Proc. Roy. Soc. A*, **245**, 312-329.

[14] Silliman, W. J. & Scriven, L. E. 1980 Separating flow near a static contact line: slip at a wall and shape of a free surface, *Journal of Computational Physics*, **34**, 287-313.

[15] Taylor, G. I. 1961 Deposition of a viscous fluid on the wall of a tube, *J. Fluid Mech.*, **10**, 161-165.

[16] Van Dyke, M. 1975 *Perturbation Methods in Fluid Mechanics*, Parabolic Press.